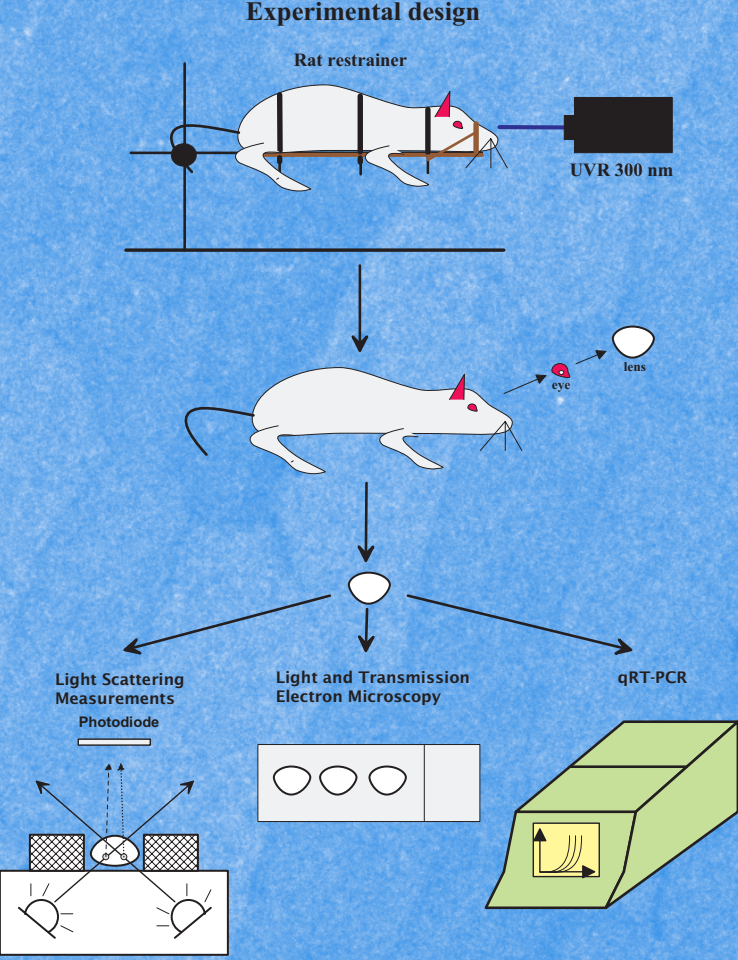


Ultraviolet Radiation Cataract



Thesis for doctoral degree (Ph.D.) 2012

Ultraviolet Radiation Cataract

Konstantin Galichanin

Konstantin Galichanin

**From the Department of Clinical Neuroscience,
St. Erik Eye Hospital,
Karolinska Institutet, Stockholm, Sweden**

ULTRAVIOLET RADIATION CATARACT

**Konstantin
Galichanin**



**Karolinska
Institutet**

Stockholm 2012

All previously published papers were reproduced with permission from the publisher.

Published by Karolinska Institutet. Printed by Universitetservice US-AB.

© Konstantin Galichanin, 2012
ISBN 978-91-7457-929-1

To my family

Life is like riding a bicycle.
To keep your balance, you must keep moving.

Albert Einstein

If

If you can keep your head when all about you
Are losing theirs and blaming it on you,
If you can trust yourself when all men doubt you,
But make allowance for their doubting too;
If you can wait and not be tired by waiting,
Or being lied about, don't deal in lies,
Or being hated, don't give way to hating,
And yet don't look too good, nor talk too wise:

If you can dream — and not make dreams your master;
If you can think — and not make thoughts your aim;
If you can meet with Triumph and Disaster
And treat those two impostors just the same;
If you can bear to hear the truth you've spoken
Twisted by knaves to make a trap for fools,
Or watch the things you gave your life to, broken,
And stoop and build'em up with worn-out tools:

If you can make one heap of all your winnings
And risk it on one turn of pitch-and-toss,
And lose, and start again at your beginnings
And never breathe a word about your loss;
If you can force your heart and nerve and sinew
To serve your turn long after they are gone,
And so hold on when there is nothing in you
Except the Will which says to them: «Hold on!»

If you can talk with crowds and keep your virtue,
Or walk with Kings — nor lose the common touch,
If neither foes nor loving friends can hurt you,
If all men count with you, but none too much;
If you can fill the unforgiving minute
With sixty seconds' worth of distance run,
Yours is the Earth and everything that's in it,
And — which is more — you'll be a Man, my son!

Rudyard Kipling

ABSTRACT

Cataract is the leading cause of blindness in the world. Epidemiological and experimental evidence supports a link between mid-range ultraviolet radiation (UVR-B) exposure and the development of cataract. Globally, there are 20 million people who have become bilaterally blind from cataract, representing 51 % of cases of all causes of blindness due to eye disease. No conservative methods are available to prevent, delay or reverse the development of cataract. The only cure for cataract is cataract surgery. A large number of people need cataract surgery, which results in a burden to the health care system. In 2004, the World Health Organization estimated that the number of cases of cataract would double by the year 2020.

The purpose of this work was to increase our understanding of acute and chronic UVR-B induced cataract development. A novel rat restrainer, a UVR source, a light dissemination meter, macroscopic imaging, light and transmission electron microscopy and quantitative RT-PCR were the methods in this thesis.

A new rat restraining device was developed to immobilize the animal and its head in order to permit a single or repeated well-controlled experimental *in vivo* exposure to optical radiation without the need for anesthesia (paper I). The newly developed rat restrainer was used in three studies: a study on the evolution of damage in the lens after a single *in vivo* close-to-threshold exposure to UV-B radiation (paper II), a study of subthreshold repeated *in vivo* exposures to UV-B radiation (paper III) and a study of GADD45 α , TP53 and CASP3 gene expression in the lens exposed to UVR-B (paper IV). In the evolution study, we characterized the chronology of morphological changes in the lens exposed to a close-to-threshold dose of UVR-B and revealed that they correlated with previously reported findings at ten times the threshold. The lens epithelium was the site of the initial UVR-B damage that progressed and subsequently involved the entire lens. Light and transmission electron microscopy revealed that epithelial damage occurred due to apoptosis within 48 hours after exposure, followed by repair at 336 hours. Cortical fiber cells remained damaged at 336 hours following exposure. In the study of subthreshold repeated *in vivo* exposures to UVR-B, daily exposures accumulated to cause cataract, supporting the epidemiological evidence for the association between solar UVR-B exposure and cortical cataract. An increase in the number of exposure days up to 30 days resulted in an increase in tolerance in the lens expressed as MTD_{2.3:16}. This finding deviates from the current safety guidelines stating that all damage in the lens is repaired within 24 hours. Double the threshold dose of UVR-B induced a transient upregulation of the stress sensor GADD45 α and a transient downregulation of the apoptosis markers TP53 and CASP3, followed by a constant upregulation of TP53 that preceded a constant upregulation of CASP3 in the rat lens *in vivo*.

Keywords: lens, ultraviolet radiation, cataract, rat, restrainer, threshold dose, apoptosis, TP53, CASP3, GADD45 α .

LIST OF PUBLICATIONS

- I. **Galichanin K**, Wang J, Löfgren S, Söderberg P. A new universal rat restrainer for ophthalmic research. *Acta Ophthalmol.* 2011 Feb; 89(1): e67-71.
- II. **Galichanin K**, Löfgren S, Bergmanson J, Söderberg P. Evolution of damage in the lens after in vivo close to threshold exposure to UV-B radiation: cytomorphological study of apoptosis. *Exp Eye Res.* 2010 Sep; 91(3): 369-377.
- III. **Galichanin K**, Löfgren S, Söderberg P. Cataract after repeated daily in vivo exposure to ultraviolet radiation. *Manuscript submitted.*
- IV. **Galichanin K**, Svedlund J, Söderberg P. Kinetics of GADD45 α , TP53 and CASP3 gene expression in the rat lens in vivo in response to exposure to double threshold dose of UV-B radiation. *Exp Eye Res.* 2012 Apr; 97(1): 19-23.

Papers not included in the thesis:

- I. Wang J, Löfgren S, Dong X, **Galichanin K**, Söderberg P. Evolution of light scattering and redox balance in the rat lens after in vivo exposure to close-to-threshold ultraviolet radiation. *Acta Ophthalmol.* 2010 Nov; 88(7): 779-785.
- II. Wang J, Löfgren S, Dong X, **Galichanin K**, Söderberg P. Dose-response relationship for α -tocopherol prevention of ultraviolet radiation induced cataract in rat. *Exp Eye Res.* 2011 Jul; 93(1): 91-97.
- III. Kronschräger M, **Galichanin K**, Ekström J, Lou M, Söderberg P. Protective effect of the thioltransferase gene on in vivo UVR-300 nm induced cataract. *Invest Ophthalmol Vis Sci.* 2012 Jan 25; 53(1): 248-52.
- IV. **Galichanin K**, Talebizadeh N, Söderberg P. Characterization of molecular mechanisms of in vivo UVR induced cataract. *J. Vis. Exp.* e4016, DOI: 10.3791/4016 (2012).

ACKNOWLEDGMENTS

Work for this thesis was performed at three universities: St Erik Eye Hospital, Department of Clinical Neuroscience, Karolinska Institutet, Stockholm, Sweden, the Gullstrand Lab, Department of Neuroscience, Uppsala University, Uppsala, Sweden and the Texas Eye Research and Technology Center, University of Houston College of Optometry, Texas, USA.

I would like to express my sincere gratitude to all who helped and supported me during the completion of this thesis, and in particular to:

Professor Per Söderberg, my main supervisor, for inviting me to do research in Sweden. I wish to thank him for introducing me to the field of ultraviolet radiation cataract, for teaching me statistics, experimental design and sharing the knowledge. His unfailing support, encouragement and guidance during the research period helped me persevere. I wish to thank him for giving me freedom in experimental work and professional development. His constructive criticism, positive attitude and enthusiasm helped me going forward in research and hunting the truth. Thank you very much!

Docent Stefan Löfgren, my co-supervisor, for his careful explanation of lab equipment and techniques. I wish to thank him for fruitful discussions, help in practical issues, scientific reasoning and friendly advices. I greatly appreciate his moral support when it was needed. For being a good friend. Thank you very much!

Professor Jan Bergmanson, for providing me the opportunity to learn transmission electron microscopy and the space in the pathology laboratory at the University of Houston College of Optometry.

Dr. Jing Wang, group member and friend, for teaching me the dissection techniques, profound discussions on various topics, her laughs and jokes in the lab.

Dr. Vino Mody, my former colleague and friend, for improving my spoken English, CV writing and preparation of the grant applications. Thanks for great tennis matches. You are the kindest person I have ever met.

Dr. Talal Ali, my mentor and friend, for great talks at St. Erik Eye Hospital during tea breaks and for inviting me to his home.

Civ. eng. Curry Bucht, Drs. Martin Kronschräger, Zhaohua Yu, Nooshin Talebizadeh and Linda Meyer, my colleagues and friends, for their collaboration and team work, scientific discussions about the lens and ultraviolet, travelling together, discovering cultural differences and similarities, and simply for the fun in the lab.

Monica Aronsson, animal care technician at St. Erik Eye Hospital, for her dedicated and unfailing help with animals.

Docent Ingeborg van der Ploeg, for scientific advices and considerations on grant application writing.

Dr. Jessica Svedlund, for teaching me PCR and her fruitful discussions and scientific advices not only at lunch and coffee times.

Lab technicians, **Berit Spångberg** at St. Erik Eye Hospital for teaching me tissue sectioning and light microscopy, **Margaret Gondo** at the University of Houston College of Optometry for her lessons on transmission electron microscopy and imaging, **Birgitta Bondeson** at Uppsala University Hospital for teaching me paraffin embedding, sectioning and staining.

Dr. Mikhail Burmakin, my friend at Karolinska Institutet, for teaching me the Western Blot technique and his generosity of time.

Drs. Milan Chromek and Igor Tomo, my friends in Stockholm, for their kind support during my research period and fantastic tough tennis matches at Karolinska Institutet Solna campus.

Drs. Oran Abdiu and Eugenio Triay, at St. Erik Eye Hospital, for all the great talks and discussions.

Dr. Olav Mäepea, colleague at Uppsala University Hospital, for being always available and his dedicated help with technical and computer issues.

Dr. Alberto Delgado Verdugo, my friend, for generous support in various life situations, scientific debates and fun inside and outside the lab. Engelberg forever!

Former and present researchers at the Centre for Clinical Medical Research at Uppsala University Hospital, **Annika Ahlford, Chuan Wang, Jessica Nordlund, Johanna Sandling, Anna-Stina Sahlqvist, Tobias Åkerström, Jonathan Hedström**, for the great talks, the company on lunches and coffee breaks and the laughers.

I thank all my friends for unbelievable times!

I express my sincerest gratitude to my family:

My dear mother, **Liudmila Örenius**, for her belief in me, my research and career. I wish to thank you cordially for all the support and encouragement when it feels so powerless. For her wise advices in life.

My dear sister, **Ksenia Galichanina**, for her positive attitude, hospitality in Stockholm and kind support in many aspects of my life.

My mother's husband, **Karl-Gunnar Örenius**, for his guidance in Swedish society and rules, his help with all kind of matters and competent advices when it is needed.

My grandmother, **Raisa Sevastjyanova**, for her continuous encouragement and cordial support.

Thank you very much!

The studies and salary were supported financially by:

EVER 2010 travel grant for the best section paper

Gun och Bertil Stohnes Stiftelse

Karin Sandqvists Stiftelse

Karolinska Institutet Foundation Grants for Eye Research

Karolinska Institutet KID-funding, faculty fund for partial financing of PhD students

Karolinska Institutet Travel Fund

Konung Gustav V:s och Drottning Victorias Frimurarstiftelse

Ögonfonden

St. Erik Eye Hospital Research Foundation

Stockholms läns landsting research grants (FoUU)

Swedish Institute Scholarship

Swedish Radiation Protection Authority

Swedish Research Council; projects K2006-74X-15035-03-2, K2008-63X-15035-05-2

Swedish Society of Medicine Travel Grant

Uppsala Läns Landsting's Research grants (ALF).

CONTENTS

1	Introduction	1
1.1	Ultraviolet radiation	1
1.2	Photoprotection	3
1.3	Ozone photochemistry and ozone depletion	4
1.4	Ocular transmittance of UVR	6
1.5	Lens structure and molecular biology	8
1.5.1	Lens capsule	9
1.5.2	Lens epithelium	9
1.5.3	Lens fiber cells	10
1.5.4	Lens transparency	11
1.5.5	Lens and cancer	12
1.6	Ultraviolet radiation cataract	12
1.6.1	Epidemiological studies	13
1.6.2	Experimental studies	14
1.7	Photochemistry and photobiology	15
1.7.1	The basic laws of photochemistry	16
1.7.2	Types of photochemical reactions	16
1.7.3	UVR photobiology	17
1.8	Toxicology	19
1.9	Maximum tolerable dose (MTD), toxicity of UVR-B to the lens	21
1.10	Apoptosis and UVR induced cataract; p53	23
2	Aims of the study	25
3	Methods	26
3.1	Experimental animals	26
3.2	Rat restrainer	26
3.3	UVR source	30
3.4	Lens dissection	31
3.5	Light dissemination meter	31
3.6	Macrophotography	32
3.7	Light and transmission electron microscopy	33
3.7.1	Protocol used for preparation for transmission electron microscopy	34
3.8	Quantitative reverse transcription polymerase chain reaction (qRT-PCR)	36
3.9	Experimental design (by papers)	37
3.10	Statistical parameters	39
4	Results and Discussion	40
4.1	Paper I, rat restrainer study	40
4.2	Paper II, evolution study of apoptotic morphological changes in the lens after exposure to UVR-B	41
4.3	Paper III, cataract after chronic repeated exposures to UVR-B	44
4.4	Paper IV, evolution study of TP53, CASP3 and GADD45 α gene expression in the lens after <i>in vivo</i> exposure to UVR-B	46
5	Conclusions	49
6	References	50

1 INTRODUCTION

1.1 ULTRAVIOLET RADIATION

The electromagnetic spectrum of ultraviolet radiation (100-400 nm) is subdivided into three regions (CIE, 1999). UVR-A (315-400 nm) contributes to premature aging of the skin and skin cancer and UVR-B (280-315 nm) has been implicated as a major source of skin cancer, sunburn and cataract; UVR-C (100-280 nm) is mutagenic but does not reach the Earth's surface due to absorption in the atmosphere by ozone and oxygen. UVR can be roughly divided based on transmission in common media. UVR-C is attenuated by the atmosphere; UVR-B is transmitted by the atmosphere but blocked by glass; UVR-A is transmitted by the atmosphere and glass. Visible radiation is in the range of 400-760 nm. Infrared or heat radiation is electromagnetic radiation with wavelengths longer than visible radiation starting at around 760 nm and ending at 1 mm.

Sunlight is the main natural source of ultraviolet radiation (Pitts, 1990). Solar irradiance incident on the Earth's atmosphere is 1367 W/m^2 (solar constant) and resembles the spectral irradiance generated by a black body radiator at 5900 Kelvin (absolute temperature of the Sun). Black body radiation is described by Planck's law according to which the spectral radiance of electromagnetic radiation depends on the temperature. Planck's law implies that intensity increases as a function of temperature and the spectral radiance shifts towards shorter wavelengths. Since a black body radiator at a certain temperature emits radiation of a known spectrum, it is commonly used as a standard for spectral calibration of optical radiation sources (Gray, 2008). The solar constant is defined as the amount of solar energy per unit area (W/m^2) incident at the outer atmosphere (extraterrestrial) at the mean earth-sun distance (one astronomical unit). The sun's rays are attenuated in the atmosphere as they pass, thus reducing the irradiance to a fraction of the solar constant, 726.9 W/m^2 , incident on a surface at sea level on a clear day (terrestrial) (Mecherikunnel et al., 1983). Sunlight on earth is defined by the Earth's insolation. Insolation is the amount of solar radiation energy received by a certain area per unit time (MJ/m^2).

Solar radiation on earth consists of 13 % UVR, 44 % visible and 43 % infrared radiation (Pitts, 1990). Global solar radiation reaches the ground directly and indirectly. Indirect solar radiation originates from light scattering, usually divided into Mie- and Rayleigh scattering. Mie, or large particle, scattering occurs when the size of the scattering volume is same or larger than the wavelength of light and is independent of volume size. Mie scattering explains the appearance of white clouds originating from the scattering of all visible spectrum wavelengths by water droplets or ice crystals in the atmosphere. Rayleigh, or small particle, scattering is the consequence when particles are smaller than the wavelength of light. The intensity of the scattered light is in Rayleigh scattering inversely proportional to the fourth power of the wavelength ($\sim\lambda^{-4}$), so that shorter wavelengths (violet and blue light) scatter much more than longer wavelengths (red and yellow light). Rayleigh scattering of sunlight in the atmosphere causes diffuse sky radiation, resulting in the blue color of the sky and the yellow color of the sun is the consequence of the loss of scattered blue light in the direct light from the sun. The reddening of the sun at sunset is also a result of Rayleigh scattering. At sunset, Rayleigh scattering increases due to the larger volume of the air that sunlight has to pass through. Thus, the scattered blue wavelength light never reaches the observer's eye. The remaining unscattered light therefore belongs to longer red wavelength light. Molecular absorption in the atmospheric gases are responsible for the absorption of solar radiation (Table 1) (Pitts, 1990).

Table 1. Spectral absorption in the solar spectrum by atmospheric gases depending on the height above the sea level.

Gas	Height (km)	Absorbed spectral band (nm)
O, O ₂ , N, N ₂	100 (Kármán line) and above	Below 85
O ₂	30-100	85-200
O ₃	30 and below	200-288

Solar infrared radiation (IRR) is not absorbed by O₂, O₃ or N₂ but is absorbed by water droplets, dust and gaseous pollutants. This is the reason why people get severe sunburn while sunbathing on an overcast day due to the

photochemical effect of UVR on the skin while IRR is blocked by the moisture in the clouds, thus giving people a false perception (Pitts, 1990).

1.2 PHOTOPROTECTION

All human beings are exposed to UVR from sunlight. All solar UVR-C and 90% of UVR-B is attenuated by atmospheric gases, whereas UVR-A is less affected by atmospheric gases. Therefore, everyone is exposed to solar UVR, mainly in the UVR-A portion and slightly in the UVR-B portion. UVR levels on the surface of the earth depend on a variety of factors. (Table 2).

Table 2. Factors influencing UVR levels on the surface of the earth.

Factor	Description
1. Sun elevation	The higher the sun in the sky, the higher the UVR level. Outside the tropics, 60% of UVR reaches the Earth between 10 a.m. and 2 p.m. in summer.
2. Latitude	UVR levels are higher closer to the equatorial region.
3. Altitude	The higher the altitude, the higher the UVR level. Each 1000 m in altitude increases the UVR level by 10%.
4. Cloud cover	The UVR level is highest on a clear sky but even overcast days provide a high UVR level.
5. Ozone	Ozone absorbs both UVR-C and some UVR-B below 288 nm. Pollution with halogens has resulted in steady ozone depletion of about 5% per decade (Madronich et al., 1998).
6. Ground reflection	Fresh snow reflects 88% of UVR-B while two day old snow reflects 50%. White sea foam reflects up to 30% of UVR-B while sea water reflects 8% of UVR-B (Slaney, 1986).

To protect people from harmful UVR, the UV index (UVI) was developed in the 1990s. The UVI was developed through a joint collaboration of the World Health Organization (WHO), the United Nations Environment Program (UNEP), the World Meteorological Organization (WMO), the International Commission on Non-Ionizing Radiation Protection (ICNIRP) and the German Federal Office for Radiation Protection. The UVI represents a measure of the

UVR level at the Earth's horizontal surface. The values are numeric from 0 to 11+. The higher the UVI, the higher the risk of harm to the skin and the eye, and the more sun protection is required. Higher UVI values decrease safe exposure time to UVR: UVI 2 permits safe sunbathing for the whole day while UVI 10 permits it for just 15 min. UVI is a unitless quantity defined by the formula (**Equation 1**).

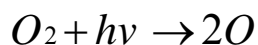
$$I_{uv} = K_{er} * \int_{250nm}^{400nm} E_{\lambda} * S_{er}(\lambda) d\lambda \quad (\text{Equation 1})$$

where E_{λ} is the solar spectral irradiance in W/m^2 at wavelength λ and d_{λ} is the wavelength interval used in the summation, $S_{er}(\lambda)$ is the International Commission on Illumination (ICE) erythema action spectrum and K_{er} is a constant equal to $40 m^2/W$.

UVI can be calculated by two methods (Verdebout, 2010). One approach is based on measurement of solar spectral irradiance with a spectroradiometer. The second approach is based on estimating the sun temperature and adopting the radiative transfer model, taking into account the total column ozone, aerosol optical thickness, surface albedo and cloud optical thickness. A strong positive linear relationship (correlation coefficient of 0.95 (Verdebout, 2010)) between measured and modeled UVR exposures permits the use of a radiative transfer computer model to predict UVI. This prediction is then announced in weather forecasts.

1.3 OZONE PHOTOCHEMISTRY AND OZONE DEPLETION

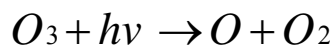
If all the ozone in the atmosphere between 15 and 50 km were compressed to the Earth's surface pressure, the layer would be only 3 mm thick. The English physicist Sidney Chapman formulated in 1930 the first photochemical theory for atmospheric ozone formation and decomposition. The chemical reactions that constitute the Chapman mechanism are as follows:



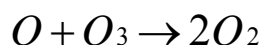
Reaction 1



Reaction 2



Reaction 3



Reaction 4

where M is any non-reactive species that absorbs the energy released in **Reaction 2** to stabilize O_3 , and $h\nu$ is the UV photon energy.

Ozone is synthesized in the stratosphere when an oxygen molecule undergoes photolysis after absorbing a UV photon with a wavelength shorter than 240 nm (**Reaction 1**). It splits the molecule of O_2 into two atoms of O. The atomic oxygen then collides with molecular oxygen to create an ozone molecule (**Reaction 2**). Ozone is not a stable molecule and falls apart to O and O_2 by photodissociation after absorbing UVR at wavelengths between 200 nm and 310 nm (**Reaction 3**). This is a continuing photochemical reaction that terminates when ozone combines with atomic oxygen to generate two molecules of oxygen (**Reaction 4**). **Reaction 1** and **Reaction 3** are chemical reactions with first order kinetics, where the rate is determined by a change in one concentration term only. **Reaction 4** is a second order kinetics reaction, where the rate is determined by a change in two concentration terms.

Reaction 2 follows third order kinetics, where the rate is determined by the variation of three concentration terms.

The global amount of ozone is defined by the balance between ozone production and destruction. The work of the scientists Paul Crutzen, Mario Molina and Sherwood Rowland in the 1970s, who were awarded the 1995 Nobel Prize in Chemistry for their work in atmospheric chemistry, particularly concerning the formation and decomposition of ozone, brought enormous attention to the environmental significance of ozone. They investigated and found that nitrous oxide (N_2O) synthesized by bacteria in soil and oceans as well as chlorofluorocarbon gases (CFCs or “freons”), used in spray bottles, refrigerators and plastic foams, damage the ozone layer. Higher consumption of nitrogen fertilizers increases production of N_2O . In fact, nitrous oxide is a major greenhouse gas and pollutant which has much more impact on global warming than carbon dioxide. Chemically inert CFCs and N_2O transported up to the ozone layer and exposed to high doses of UVR

yield reactive atoms which react with ozone and destroy it, resulting in ozone depletion. Ozone depletion in turn shifts the UVR absorbance to shorter wavelengths with higher energy and more harmful photons.

During the past 100 years, the concentration of ozone in the lower layers of the atmosphere has increased causing more heat transfer to the earth surface due to absorption of sun radiation, while simultaneously pollution by nitrous oxide, carbon dioxide and CFCs have increased the consumption of ozone in the higher layers, resulting in a global net decrease of ozone, allowing more UVR to reach the earth surface.

Global ozone depletion is estimated at about 5 % per decade (Madronich et al., 1998). A new model for the prevalence of cortical cataract has estimated that with 5-20 % of ozone depletion, there will be 167,000-830,000 additional cases of cortical cataract in the American population by 2050 (West et al., 2005).

1.4 OCULAR TRANSMITTANCE OF UVR

Light incident on the eye is transmitted to the retina travelling through several optical media: the cornea, aqueous humor, crystalline lens and vitreous body (Figure 1, Figure 2).

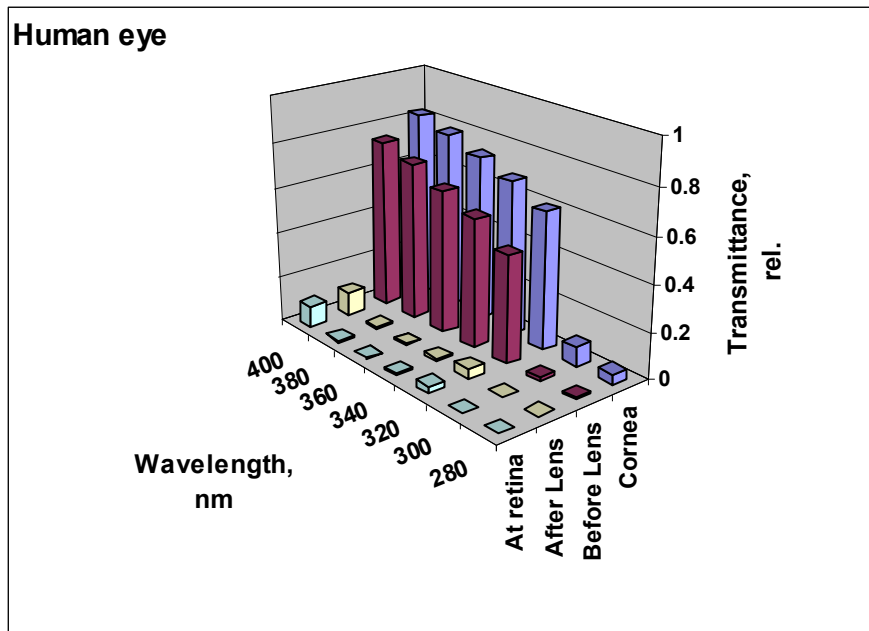


Figure 1. Transmittance of the human eye for UVR (Boettner and Wolter, 1962).

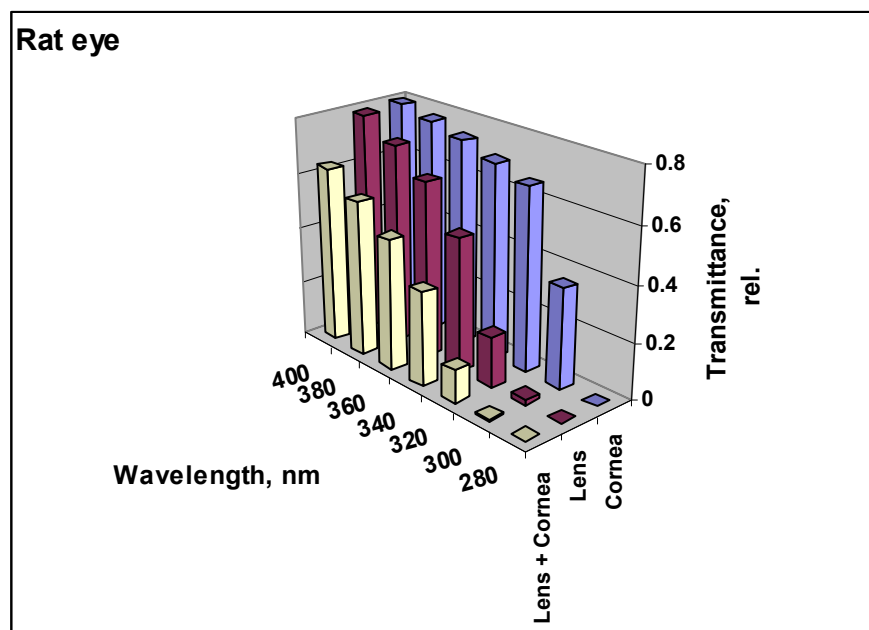


Figure 2. Transmittance of rat cornea (Dillon et al., 1999) and rat lens (Gorgels and van Norren, 1992) for UVR.

Corneal absorption is a mayor contributor to UVR protection of the intraocular optical components.

The human cornea attenuates 92 % of UVR at 300 nm and 18 % of UVR at 400 nm (Boettner and Wolter, 1962), whereas the rat cornea attenuates 64 % of UVR at 300 nm and 20% of UVR at 400 nm (Dillon et al., 1999). This indicates that corneal transmittance is species- and wavelength-dependent in addition to thickness dependence.

Boettner et al. (Boettner and Wolter, 1962) observed in nine human eyes at the ages of 4 weeks, 2, 4.5, 23, 42, 51, 53, 63 and 75 years that ocular media in the human eye absorb essentially all UVR from 280 nm to 400 nm, except rays of UVR reaching the retina at 320 nm (3%) and at 400 nm (9%).

Although the data presents the mean transmittance with a sample size of nine subjects and different age categories, the results also reveal that the lens of a child under 5 years of age transmits about 8% of UVR at 320 nm, while that of a 22 year old man transmits less than 0.1% of UVR at this wavelength (Boettner and Wolter, 1962).

1.5 LENS STRUCTURE AND MOLECULAR BIOLOGY

The vertebrate ocular lens is suspended in the eyeball, situated behind the cornea and iris, and is supported posteriorly by the vitreous body. The slightly convex anterior surface of the lens is in contact with the pupillary margins of the iris, and its more convex posterior surface occupies the saucer-shaped depression of the vitreous body called the hyaloid fossa. The primary support of the lens is provided by suspensory ligaments, known as zonular fibers, which originate from and are produced by the ciliary body and integrate into the equatorial rim of the lens. Contraction and relaxation of the ciliary muscles modify the tension of the zonular fibers, changing the shape of the lens for near and far vision, respectively. This is the basic principle of accommodation: focusing of the lens to give a clear view of a specific object.

The lens consists entirely of densely packed lens fiber and epithelial cells, enclosed by a thick lens capsule. An orderly alignment of the elongated fiber cells, which extend circumferentially from anterior to posterior, make up the mass of the lens. The fiber cells are arranged in many layers and comprise 95% of the tissue volume. Fiber cells in the same layer, but running in diametrically opposite meridians, meet end to end along radial planes known

as lens sutures. Beneath the capsule, the anterior surface is covered by a monolayer of cuboidal cells, the lens epithelium.

1.5.1 Lens capsule

The lens capsule is composed primarily of collagen IV and laminin networks together with nidogen and perlecan. All four molecules and water form a viscoelastic membrane that provides the structural and functional basis for lens accommodation (Danysh and Duncan, 2009). Other molecules such as the glycoprotein fibrillin contribute to the structure of the capsule. Fibrillin appears in the zonular lamella, the place in the lens capsule where the zonules insert into the capsule (Mir et al., 1998); (Streeten, 1977). Mutation in the FBN1 gene results in Marfan's syndrome, an autosomal dominant connective tissue disorder, clinically manifested by lens dislocation.

The lens capsule separates the lens from other ocular tissues, thereby serving as a barrier. The anterior lens capsule is thicker than the posterior. For instance in the electron microscope microscopy, the rat lens capsule measures about 10 μm at the anterior pole and 5 μm at the posterior pole (Galichanin et al., 2010). The lens capsule is an immune privileged site and is not permeable to bacteria, many viruses and other cells. It has been reported that crystallins (50-900 kDa) and DNA plasmids can transit through the lens capsule, with and without pre-encapsulation in liposomes (Boyle et al., 2002). The largest pores in the lens capsule are about 25 nm in diameter, whereas the majority of pores are about 8 nm or smaller (correspondence with Professor M. Duncan).

1.5.2 Lens epithelium

The lens epithelium is divided into four zones: the central zone (80% of the lens epithelium surface area), the pregerminative zone (5%), the germinative zone (10%) and the transitional zone (5%), independent of age. The central zone epithelial cells are in the resting phase (G_0) after the cell cycle checkpoint in the G_1 phase and do not differentiate into fiber cells (Harding et al., 1971). The pregerminative zone epithelial cells are located peripherally to the central zone. They enter into M phase when needed to increase the number of epithelial cells due to growth and aging (Rafferty and Rafferty,

1981). Periferal to the pregerminative zone is the germinative zone that comprises cells that undergo mitosis, providing pairs of daughter cells. Daughter cells terminally differentiate into secondary fiber cells. The number of daughter cells produced is greater than the number of secondary fiber cells (Rafferty and Rafferty, 1981), which indirectly leads to the conclusion that some daughter cells might become epithelial cells and add to the epithelial cell population. It is also possible that some cells are eliminated. The self-renewal property and potency of epithelial cells in the lens germinative zone resembles somatic stem cells. The transitional zone epithelial cells, peripheral to germinative zone cells, have already begun fiber cell elongation.

The total number of epithelial cells in primates increases with age with a peak in adulthood which then decreases from adulthood to elderness. Central zone epithelial cell numbers are 287,701 at birth and 290,696 in old age, but the number of epithelial cells in the germinative zone doubles from 121,718 at birth to 254,744 in old age. The increased size of epithelial cells in the central zone with age is more notable than in the germinative zone. The size of epithelial cells in the central zone in old age in primates is 2.5 times larger than at birth, whereas the size of epithelial cells in the germinative zone in old age is 1.3 times larger than at birth. Such zonal variation reveals that the germinative zone constantly increases its cell population whereas the central zone cell population grows throughout adulthood and decays in old age (Kuszak and Costello, 2004).

1.5.3 Lens fiber cells

The cross-section of a fiber cell demonstrates its hexagonal prism shape. Fiber cells differentiate and go through several stages: elongation, maturation and mature fiber cell differentiation. The transitional zone cells migrate posteriorly, rotate 90° about their polar axis and start to elongate in both directions, with one end moving toward the anterior pole and the other end moving toward the posterior pole, in response to fibroblast growth factor (FGF) secreted by the retina (Lovicu and McAvoy, 2005). Elongating fiber cells have smooth membranes and direct contact with the capsule and the epithelium at their basal and apical surfaces, respectively. Protein synthesis

and storage increase during fiber cell elongation. When elongating fiber cells lose their contacts with the epithelium and capsule, they have completed the process of elongation and enter the next stage as maturing fiber cells. New basal-basal and apical-apical contacts are created between fiber cells from opposite sides of the lens which results in lens suture formation. As fiber cell ends reach these sutures, the lateral membranes become more tightly interconnected forming “ball-and-socket junctions” (Kuszak et al., 1980). Fiber cells start losing their organelles in the presence of proteases and nucleases, resulting in the formation of an organelle-free zone (Bassnett and Beebe, 1992; Kuwabara, 1975). Fiber cells that fill the organelle-free zone (OFZ) are called mature fiber cells. Shestopalov et al. utilized plasmid technology and confocal microscopy to determine that fiber cells are transcriptionally and translationally competent until the time of organelle loss (Shestopalov and Bassnett, 1999). Microinjection of pDNA encoding GFP into lens fiber cells localized at various lens depths revealed that deepest GFP-synthesizing fiber cell was located just before the OFZ (Shestopalov and Bassnett, 1999).

1.5.4 Lens transparency

The lens is a unique tissue due to its transparency. The transparency of the crystalline lens is dependent on the regular order of its cells, organelles and proteins.

Mature fiber cells are located on the visual axis of the lens where there are no organelles. Cell organelles potentially cause Mie scattering. Their absence on the optical axis contributes to transparency. Interestingly, the refractive index of the fiber membranes in the lens nucleus is approximately the same as that of the fiber cytoplasm in the lens nucleus (Michael et al., 2003), which makes light scattering in the lens nucleus negligible. In addition, the concentration of proteins in the cytoplasm of the lens nucleus is two or three times higher than in the lens cortex, thus the refractive index in the cytoplasm of nuclear fiber cells is higher than in the cortical fiber cells. This gradient in refractive index serves to correct the lens for longitudinal spherical aberration.

The lens functions as a syncytium. It has multiple cell-cell fusions between fiber cells. Cortical fiber cells have gap junctions that are permeable to ions and other small molecules (Kuszak et al., 1978). Microinjection of plasmid vectors encoding GFP into individual fiber cells in chicken eggs results in GFP expression in injected fiber cells, followed by the spread of GFP throughout the lens core (Shestopalov and Bassnett, 2000). These data show that nuclear fiber cells develop cell-to-cell connections capable of protein passage. These cell interconnections in the core of the lens might equalize the protein concentrations between fiber cells, thus decreasing differences in the refractive indices between neighboring cells. This reduces internal light scattering which enhances the transparency of the lens core.

1.5.5 Lens and cancer

There are no nerves or blood/lymphatic vessels in the lens. The anaerobic ambient in the lens, the lack of a vasculature and the thick capsule with pores impermeable to cells may explain the absence of cancer of the lens. There have been case reports of cataract caused by choroidal melanoma (Shen et al., 2007) and posterior capsule opacity as a clinical manifestation of metastases of skin melanoma (Solomon et al., 2011). However, tumor cell penetration through the lens capsule has not been observed. On the other hand, the parasite *Diplostomum spathaceum* can transit through the lens capsule in fish since the parasite has a trypanocytic organ, or attachment organ, that secretes proteolytic enzymes to lyse biological membranes (Höglund, 1999).

1.6 ULTRAVIOLET RADIATION CATARACT

Cataract is the leading cause of blindness in the world (Thylefors, 2001). There are estimated to be almost 20 million people who have become bilaterally blind from cataract, representing 51 % of all causes of blindness due to eye diseases globally. Thus, cataract remains the leading cause of blindness (WHO, 2010). The number of cases of cataract will double by the year 2020 as projected by the World Health Organization (Brian and Taylor, 2001). No conservative methods are available to prevent, delay or reverse the

development of cataract. The only cure for cataract is cataract surgery. In developed countries, the most common surgical technique is ultrasonic phacoemulsification. Due to a shortage of ultrasound machines in developing countries, extracapsular cataract extraction is still the operation of choice. A large number of people need cataract surgery, which is a burden on the health care system. A delay in cataract onset of 10 years would reduce the need for cataract surgery by 50% (Congdon, 2001).

WHO defines cataract as clouding of the lens of the eye which impedes the passage of light. Cataract is primarily an age-related disease. There are several risk factors contributing to the development of cataract including smoking, diabetes mellitus, ultraviolet radiation, alcohol, ionizing radiation and hypertension (West and Valmadrid, 1995). A reduction in tobacco smoking, exposure to sunlight and alcohol consumption therefore should decrease the prevalence of cataract.

1.6.1 Epidemiological studies

The prevalence of cortical cataract is higher at lower latitudes since these regions have a higher UVR level, as concluded by a comparative study of three epidemiological surveys in Reykjavik, Melbourne and Singapore (Sasaki et al., 2003). This study also reported that the location of the cortical opacification is more pronounced in the lower nasal quadrant of the lens. Other quadrants of the lens are protected from direct and albedo radiation by the pupil and the facial skeleton. Moreover, the frontal section of the cataractous lens exhibits abundant opacifications on the equator of the lens. This was explained by the Coroneo theory of albedo, i.e. indirect radiation, and its concentration on the periphery of the lens (Coroneo et al., 1991). The higher concentration of UVR at the lens equator results in irradiation of the germinative zone of the lens which is comprised of epithelial cells that are presumably more sensitive to UVR damage.

Epidemiological data indicates an association between exposure to UVR-B from the sun and the development of cortical cataract (McCarty and Taylor, 2002). A dose-response relationship was reported in studies which evaluated the link between latitude and the prevalence of cataract (Sasaki et al., 2003).

A cross-sectional Chesapeake Bay study of 838 watermen found an association between the degree of solar UVR-B exposure and cortical cataract. Subjects with cortical cataract had a 21 % higher exposure to UVR-B in every year of life after the age of 15, suggesting that damage to the lens is cumulative. The study did not reveal a link between UVR-B exposure and nuclear cataract or between UVR-A exposure and cataract (Taylor et al., 1988). Another cross-sectional study, the Beaver Dam Eye Study, showed a relationship between exposure to UVR-B and cortical cataract that was significant only in men (Cruickshanks et al., 1992).

Drawbacks of epidemiological studies are difficulties in the measurement of individual ocular UVR-B exposure and quantification of clinically relevant cataract. Further, epidemiology does not allow derivation of an action spectrum for UVR induced cataract, nor the pathophysiological mechanism. Therefore experimental studies were required.

1.6.2 Experimental studies

Experimental evidence links UVR-B exposure and the development of cortical cataract (Hightower, 1995a; Söderberg, 1988; Wang et al.). The lens has a maximum sensitivity to UVR at wavelengths around 300 nm (Merriam et al., 2000; Pitts et al., 1977). Qualitative investigation of the action spectrum for cataract formation in the rabbit by Pitts et al. (Pitts et al., 1977) revealed that the wavelength region around 300 nm is the most cataractogenic. Later a quantitative study on rat lenses by Merriam et al. (Merriam et al., 2000) confirmed that the lens is most sensitive to UVR exposure at 300 nm.

The homeostasis in which the lens develops, differentiates and grows throughout life is maintained the lens. The structure-function regimen of the lens is impaired by UVR (Zigman, 1985). UVR-B photons damage both the lens epithelium and lens fiber cells by different mechanisms, respectively. The lens epithelium is the first target for UVR-B that is transmitted by the cornea. In lens epithelial cells, UVR-B irradiation leads to unscheduled DNA synthesis (Söderberg et al., 1986), the formation of pyrimidine dimers, DNA-DNA and DNA-protein cross-linking, DNA single and double strand breaks (Kleiman et al., 1990), perturbation of calcium cell signaling and a decline in reduced glutathione (Hightower et al., 1999) (Wang et al.), Na/K-ATPase

inhibition (Hightower and McCready, 1992), increased membrane permeability (Hightower et al., 1994) and alterations in protein synthesis (Andley et al., 1990). Damage by UVR to the epithelium is mediated to underlying lens fiber cells by an increase in the calcium concentration (Hightower, 1995b). In lens fiber cells, UVR-B causes the aggregation of lens crystallins (Zigman et al., 1973), photolysis of human lens α -crystallin and the generation of reactive oxygen species (Andley and Clark, 1989), mitochondrial rounding and movement cessation (Bantseev and Youn, 2006). In addition, apoptosis has been studied extensively in UVR induced cataract *in vitro* (Li and Spector, 1996). In our research group, studies on transmission electron microscopy of rat lenses after *in vivo* exposure to UVR-B showed apoptosis in lens epithelial cells (Michael et al., 1998b). Quantitative RT-PCR investigations revealed that UVR-B exposure increases the mRNA expression of apoptosis markers p53 and caspase-3 in the rat lens (Ayala et al., 2007). All mechanisms of UVR induced lenticular damage lead to an increase in light scattering in the lens.

To measure light scattering in the lens, Söderberg developed an objective method for light scattering measurement using a light dissemination meter (Söderberg et al., 1990). This method established the 95 % tolerance limit for non-pathological light scattering as 0.35 tEDC, which can be used as a threshold in binary and continuous dose-response functions. The light dissemination meter was then employed in the evolution study of *in vivo* exposure of rat lenses to UVR at 300 nm (Söderberg, 1990). This study demonstrated an increase in the difference in light scattering between exposed and unexposed lenses with an exponential decline towards an asymptote as a function of time (Söderberg, 1990).

1.7 PHOTOCHEMISTRY AND PHOTOBIOLOGY

Photochemistry is a sub-discipline of chemistry, and is study of the chemical reactions that occur under the effect of visible and ultraviolet radiation.

Longer wavelengths, e.g. infrared, cause vibrational excitation of molecules, resulting in thermal damage. Photochemistry is the underlying mechanism for all photobiology. When a molecule absorbs a photon of light, its electronic

structure changes, moving electrons to higher energy orbitals, such that the molecule reacts differently with other molecules. The electromagnetic energy that is absorbed from light can result in photochemical changes in the absorbing molecule, i.e. a *direct phototoxic reaction*, or in an adjacent molecule, i.e. an *indirect photosensitized reaction*. In the indirect photosensitized reaction, absorbed photon energy excites an energy-transmitting molecule, a *photosensitizer*, which transfers energy to an adjacent molecule. The energy can be emitted as heat, or as lower energy light, i.e. *fluorescence or phosphorescence*, in order to return the molecule to its ground state.

1.7.1 The basic laws of photochemistry

The first law of photochemistry, the *Grotthuss-Draper law*, states that light must be absorbed by a chemical substance in order for a photochemical reaction to take place. If electromagnetic energy is not absorbed, no photochemistry will occur and no photobiology will be observed.

The second law of photochemistry, the *Stark-Einstein law*, states that for each photon of light absorbed by a chemical system, only one molecule is activated for a photochemical reaction. This law is true for ordinary light intensities, but with high-power lasers, two-photon reactions can occur.

The *Bunsen-Roscoe law of reciprocity* states that a photochemical effect is directly proportional to the total energy dose, or number of photons, irrespective of the time in which the dose is delivered. Ayala et al. disqualified the law of reciprocity for UVR induced cataract in albino rats (Ayala et al., 2000). Ayala found that for exposure durations up to 60 minutes there was a maximum sensitivity around 15 minutes at equivalent total energy dose. The lack of reciprocity was probably due to biological modulation of the primary photochemical reaction.

1.7.2 Types of photochemical reactions

1. *Linear addition to an unsaturated molecule*, e.g. the nucleobase thymine in DNA can react with the amino acid residue cysteine in

proteins. This photochemical reaction occurs in UVR crosslinking of DNA and proteins.

2. *Cycloaddition of unsaturated molecule*, e.g. two thymines can combine to create a ring product, the thymine dimer, a product formed in DNA by UVR.
3. *Photofragmentation*, e.g. the side chain of riboflavin can split to lumiflavin and lumichrome. Lumiflavin and lumichrome act as photosensitizers in UVR-A induced cross-linking between riboflavin triplets and reactive groups of corneal proteins (Kamaev et al.). UVR-A induced corneal cross-linking with riboflavin is used in the treatment of corneal ectasia in keratoconus and post-LASIK ectasia.
4. *Photooxidation*, e.g. the ring structure of cholesterol can add a peroxy group.
5. *Photohydration*, e.g. uracil can add a molecule of water after UVR exposure.
6. *Cis-trans isomerization*. This occurs when the 11-cis-retinal chromophore absorbs a photon, whereupon it isomerizes to all-trans-retinal in the process of phototransduction in the eye retina. The absorbance spectrum of the chromophore depends on its interaction with the opsin protein in photoreceptor cells.
7. *Photorearrangement*. This photochemical reaction occurs in the skin when 7-dehydrocholesterol absorbs solar UVR-B around 297 nm and is converted to vitamin D₃.
8. *Energy transfer* occurs in all photosensitized reactions. One of the applications of photosensitized reactions in the clinic is photodynamic therapy of age-related macular degeneration and cancers. When an oxygen molecule and photosensitizer are in proximity, energy transfer can occur that results in the photosensitizer converting into its ground singlet state and creating excited singlet state oxygen. In turn, singlet oxygen causes oxidative stress to tumor cells. In age-related macular degeneration, photosensitization destroys abnormal blood vessels in the retina.

1.7.3 UVR photobiology

Photobiology is the study of how electromagnetic radiation interacts with living matter (Pitts et al., 1986). UVR causes photochemical alterations in DNA, RNA, proteins and lipid fatty acids. DNA is one of the most important targets of damaging UVR. DNA is the largest molecule in the cell. It is not present in many copies like RNA and proteins. It carries the genetic information of the cell and it absorbs UVR efficiently. UVR-induced direct damage includes the modification of individual purine and pyrimidine bases, the production of pyrimidine dimers and the addition of other molecules to nucleobases (DNA-protein cross-linking). UVR-induced indirect damage to DNA results in single and double DNA strand breaks as the consequence of DNA repair (nucleotide excision repair). However, ionizing radiation has more photon energy than non-ionizing ultraviolet radiation and thus can directly break DNA strands. The terminal deoxynucleotidyl transferase dUTP nick end labeling (TUNEL) assay can be utilized to detect DNA strand breaks.

Ultraviolet radiation can also induce mutations, i.e. alterations in the DNA base sequence of a gene as consequence of defect repair. DNA damage and mutation are two different major types of DNA error. Mutations cannot be repaired because a base change in both DNA strands cannot be identified by enzymes, whereas DNA damage is repairable. If DNA damage is not repaired, it can kill the cell by blocking replication or it can cause DNA replication errors, a major source of mutations. In slowly dividing cells, unrepaired DNA damage may accumulate over time. In contrast, in rapidly dividing cells, unrepaired DNA damage causes mutations. Mutations that confer survival properties to frequently dividing cells have a carcinogenic effect.

The cell has a repair system to protect against DNA damage. Important repair mechanisms are photoreactivation, base excision repair, nucleotide excision repair, recombinational repair and double-strand break repair. Some DNA repair mechanisms produce mutations, but others are accurate and do not produce mutations.

1.8 TOXICOLOGY

Toxicology can be defined as a discipline of science that studies the harmful effects caused by poisons or physical phenomena, such as radiation.

Ultraviolet radiation causes toxicity in biological tissue. Toxicity can be *acute* or *chronic*. Acute toxicity is defined as toxicity elicited immediately following short-term exposure. In other words, acute exposure results in an immediate effect. In contrast to acute toxicity, chronic toxicity is mediated by continuous exposure and sublethal effects. Acute toxicity typically occurs at high doses in contrast to chronic toxicity which occurs at doses below those that induce acute toxicity.

Acute toxicity is quantified by its dose-response function. A dose-response function represents the causal relationship between the dose of an agent and the response to that agent. A dose response may be *binary* and *continuous*. If the dose-response is binary, the response is defined as “event” or “no event” without any grade. A binary response follows a binomial distribution with a defined probability for the event. If the dose-response is continuous, it is however convenient to define a significant response, e.g a threshold, based on the quantitative data. If the continuous dose-response function can be mathematically modeled, the parameters for the regression can be estimated with regression allowing estimation of the threshold dose.

When the continuous dose-response function of a normally distributed response is plotted, the curve is sigmoidal in shape (Figure 3).

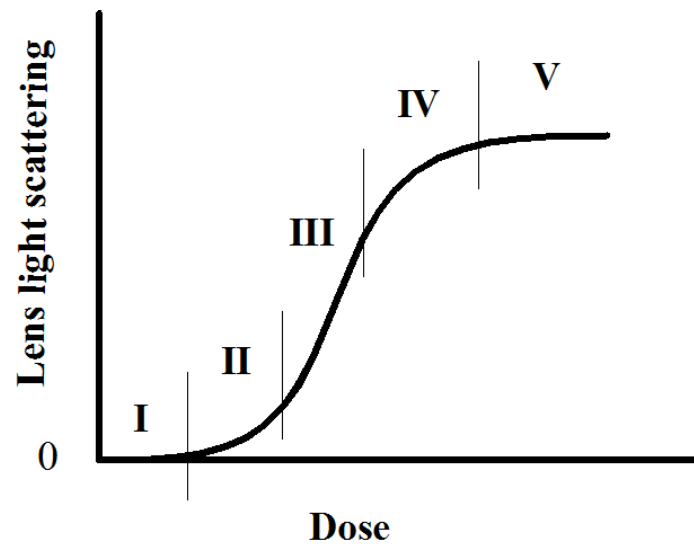


Figure 3. The sigmoidal dose-response curve with five segments.

An often applied strategy in experiments on UVR-B induced cataract, is to define the response as the difference in forward light scattering between UVR-B exposed and unexposed lenses. The dose-response curve can be divided into five segments:

Segment I. This segment does not have any slope; there is no increase in difference in forward lens light scattering when the dose increases.

Segment II. This portion represents those doses of UVR-B that induce a difference in forward light scattering that increase exponentially with dose.

Segment III. This segment consists of doses of UVR-B that induce an approximately linear increase in light scattering. It is the steepest among the segments.

Segment IV. This portion represents those doses of UVR-B that induce a difference in forward light scattering that increase with an exponential decline with dose.

Segment V. This segment has no slope and represents doses that exceed the maximum damage that can be expressed.

The dose-response curve can be used to estimate the threshold dose. The *threshold dose* refers to the dose of an agent below which a significant effect does not occur and above which a significant effect occurs. Threshold dose is empirically estimated as a dose less than the lowest dose at which a

significant effect is detected but higher than the greatest dose at which no effect is detected. (Figure 3).

The slope of the linear regression for a dose-response curve in *Segment III* (Figure 3) is reflected by the regression coefficient. A higher regression coefficient makes the slope steeper. The slope can provide valuable information on the specificity of the agent in the interaction with the biological substance. Steep slopes for the dose-response line are characteristic of toxicants that induce toxicity by interacting with a specific target in the tissue, while shallow slopes are characteristic of toxicants that induce more non-specific toxicity.

1.9 MAXIMUM TOLERABLE DOSE (MTD), TOXICITY OF UVR-B TO THE LENS

The current safety limits for the avoidance of UVR-B induced cataract are provided by the International Commission for Non-Ionizing Radiation Protection (ICNIRP). The latest ICNIRP guideline on limits of exposure to ultraviolet radiation of wavelengths between 100 nm and 400 nm was published in 2004. Permissible levels of exposure to UVR in this guideline are based on animal and epidemiological studies and accumulated experience on use of the previous guideline. The fundamental experiment, on pigmented rabbit eyes for the avoidance of UVR induced cataract by Pitts et al., is based on the binary dose-response model with “cataract” and “no cataract” as outcome (Pitts et al., 1977). The threshold dose was measured to be 1.5 kJ/m² for transient cataract and 5 kJ/m² for permanent cataract (Pitts et al., 1977). However, a study on albino rats in our group concluded that UVR-B induced cataract follow a continuous dose-response function (Söderberg et al., 2003).

As consequence, a new strategy was developed for estimation of threshold dose for continuous dose response functions, maximum tolerable dose (MTD) (Söderberg et al., 2002). The explanatory variable for the dose-response function in the MTD concept is the dose while the response variable is the paired difference in forward light scattering between exposed and contralateral unexposed lenses (Figure 4).

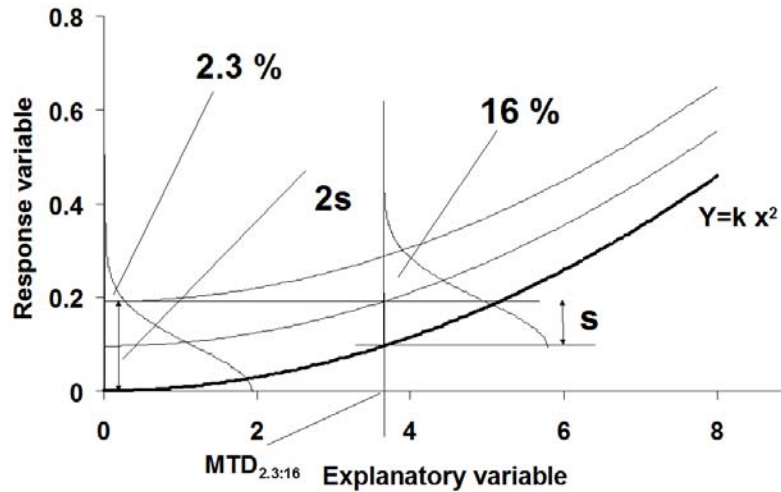


Figure 4. Definition of $MTD_{2.3:16}$.

Measurements of difference of light scattering between sides within subjects are associated with measurement error and variation among subjects. For analysis of measurement data, it is therefore necessary to include an error term in the response as a function of the explanatory variable. It is advantageous if the error term is normally distributed with an expected mean of 0 and an expected standard deviation. Then, the probability of finding a difference in lens light scattering in a population of unexposed rats at two standard deviations ($2s$) above 0 is 2.3 % (Figure 4). This difference in light scattering is the *tolerance limit for normality*. Furthermore, the probability of finding a difference in lens light scattering between exposed and unexposed lenses one standard deviation (s) above the dose-response function is 16 % (Figure 4). This is the *criterion for significant toxicity*. The MTD is then defined as the dose that corresponds to the crossover between the tolerance limit for normality and the criterion for significant toxicity. An individual exposed to MTD has a 16 % probability of showing a difference in forward light scattering between exposed and unexposed lenses greater than what would be found in 97.7 % of unexposed individuals (Figure 4). The $MTD_{2.3:16}$ for six-week-old albino rats in this experiment was estimated to be 3.65 kJ/m^2 . Later, $MTD_{2.3:16}$ for acute UVR-B cataract was determined to be for pigmented mouse 2.9 kJ/m^2 (Meyer et al., 2008), for pigmented rat 4.2 kJ/m^2 (Kakar et al., 2003) and for pigmented guinea pig 69 kJ/m^2 (Mody et al.). The lens of the pigmented guinea pig is the most tolerant to UVR at 300 nm among the species studied in our group.

1.10 APOPTOSIS AND UVR INDUCED CATARACT; p53

Apoptosis is known as programmed cell death. The term apoptosis was introduced by Kerr et al. in 1972 to describe the morphological changes of the programmed cell death that occurs under physiological conditions and as a result of external stimuli (Kerr et al., 1972). Transmission electron microscopy is the gold standard to demonstrate apoptosis and differentiate it from necrosis. Microscopically, apoptosis is described as the condensation of nuclear chromatin (karyopyknosis), followed by segmentation of the nucleus (karyorhexis) and cell disintegration into apoptotic bodies containing cellular material. Finally, apoptotic bodies are taken up by macrophages or adjacent cells and digested within phagolysosomes (Elmore, 2007). There is no inflammatory reaction in apoptosis, in contrast to necrosis, because apoptotic cells do not release their cellular material into the intercellular space and are quickly phagocytized by surrounding cells (Kurosaka et al., 2003).

Biochemically, there are two well-understood pathways: the extrinsic or death receptor pathway and the intrinsic or mitochondrial pathway. There is an additional pathway that involves T-cell mediated cytotoxicity. These three pathways converge on the same terminal or execution pathway. This pathway is initiated by the cleavage of caspase-3 which in turn activates the endonuclease CAD which degrades chromosomal DNA and causes chromatin condensation. Therefore, caspase-3 is a reliable marker of apoptosis with better specificity than the TUNEL assay (Duan et al., 2003; Gown and Willingham, 2002; Walker and Quirke, 2001).

One of the mechanisms involved in cataract formation in humans and animals is apoptosis (Li et al., 1995). UVR-B induces apoptosis in lens epithelial cells *in vitro* (Li and Spector, 1996). Our group studied UVR-B induced apoptosis in the lens *in vivo* (Michael et al., 1998b). Ayala et al. studied the expression of p53 mRNA and protein in lenses exposed to UVR-B *in vivo* and revealed that exposed lenses exhibit increased expression of both (Ayala et al., 2007).

The p53 protein is a cancer suppressor in humans and is encoded by the TP53 gene. It is one of the most commonly mutated genes, with about 50% of cancers containing TP53 mutations (Soussi and Beroud, 2001). In unstressed

cells, active p53 is kept at a low concentration with a short half-life (20 minutes) (Levine, 1997). The protein Mdm2 binds to newly synthesized p53 and represses its activity by promoting degradation by polyubiquitination (Coutts et al., 2009), thus blocking p53 transcriptional activation. Stress signals lead to the dissociation of Mdm2-p53 complex and therefore activation of p53. Consequently, p53 binds to DNA as a tetramer in a sequence-specific manner that results in the transcriptional regulation of genes involved in DNA repair, cell cycle arrest, apoptosis and senescence (Riley et al., 2008). In response to DNA damage that cannot be repaired, p53 activates the transcription of genes that encode the pro-apoptotic Bcl2 proteins which in turn trigger the mitochondrial pathway of apoptosis (Schuler and Green, 2001). p53 can play a role in apoptosis through a transcription-independent mechanism where p53 accumulates during stress to control mitochondrial-directed apoptosis. This mechanism is carried out by Mdm2-mediated monoubiquitination of p53 that promotes the transport of p53 to the mitochondria (Marchenko et al., 2007). However, some studies have revealed that p53 is not required to induce apoptosis (Clarke and Clarke, 1996; Zhuang et al., 1995). To investigate the role of p53 in UVR-B induced apoptosis in the lens, we studied the time course of the onset of p53 and caspase-3 mRNA expression in the lens after *in vivo* exposure to UVR at 300 nm.

2 AIMS OF THE STUDY

The aims of this thesis were:

- I. To develop a rat restrainer that immobilizes the head of an unanesthetized animal to allow single and repeated controlled experimental *in vivo* exposure to optical radiation.
- II. To investigate whether the morphology and chronology of cataract developement after close-to-threshold UVR at 300 nm is similar to that at ten times the threshold.
- III. To elucidate the cumulative cataractogenic effect of repeated subthreshold UVR-B exposures to the lens.
- IV. To study the time course of mRNA expression of the stress sensor and DNA repair gene GADD45 α , TP53 and the apoptosis marker CASP3 in the rat lens *in vivo* after exposure to UVR at 300 nm.

3 METHODS

3.1 EXPERIMENTAL ANIMALS

Six-week-old and eighteen-week-old female Sprague-Dawley albino rats were used as the experimental animals. All animals were obtained from a commercial breeder (Scanbur BK AB, Sollentuna, Sweden). All animals were treated in accordance with the *ARVO Statement for the Use of Animals in Ophthalmic and Visual Research*. Ethical approval was obtained from Northern Stockholm Animal Experiments Ethics Committee. Ethical approval protocol numbers were N184/04 (papers I and II) and N187/07 (papers III and IV).

The Sprague-Dawley rat was selected as the experimental animal because the *in vivo* response to UVR at 300 nm is well-characterized in this animal model (Michael et al., 1998a); (Ayala et al., 2000); (Merriam et al., 2000); (Söderberg et al., 2002). Moreover, this animal was chosen because it is available at a uniform size in large numbers at affordable price. The gender of rats was selected to be female because, in contrast to males, females have less allergenic urine. There is no difference between sexes in relation to severity of UVR cataract (Löfgren et al., 2003). Albino rats are more sensitive to UVR-B than pigmented rats, as shown in a recent publication by our group (Löfgren et al., 2012).

The age was chosen to be six weeks for Sprague-Dawley rat in papers I, II and IV because our group has gained extensive experience with rats of this age. The $MTD_{2.3:16}$ concept was introduced in six-week-old Sprague-Dawley rats (Söderberg et al., 2002). The age of the 18-week-old rats in papers I and III was selected because $MTD_{2.3:16}$ for the avoidance of UVR cataract for rats at the age of 18 weeks and above does not change (Dong et al., 2005). Thus, for rats aged 18 weeks and above, age does not change the $MTD_{2.3:16}$.

3.2 RAT RESTRAINER

The idea of developing a rat restrainer came to us when we planned an *in vivo* study of daily repeated exposures to UVR-B. General anesthesia is the most common method to immobilize animals in experimental research. Ketamine and xylazine are commonly used in combination for the narcosis of animals (Dong, 2005); (Ayala, 2005); (Mody, 2008). However, there are side effects of anesthetics that do not allow long-term daily experiments. Marietta et al. revealed that chronic ketamine administration in low doses resulted in a two-fold increased rate of N-demethylation of ketamine, a marker for the liver microsomal cytochrome P450 (Marietta et al., 1976). In addition, disturbances in hepatic and renal function were found after 40 min and 5 days following anesthesia in guinea pigs (D' Alleinne and Mann, 1982). General anesthesia also produces ocular side effects such as “acute reversible lens opacities” (Calderone et al., 1986; Fraunfelder and Burns, 1962, 1970), keratoconjunctivitis sicca (Kufoy et al., 1989) and anterior uveitis (Kufoy et al., 1989). The combination of ketamine and xylazine causes acute transient cataract in albino rats (Zhang et al., 2007). Restraining devices, previously developed (Caul and Buchanan, 1971; Lewis et al., 1989; Pitts, 1976; Rice and Ketterer, 1977; Warden et al., 2000) and commercially available, do not adequately fixate the animal's head, and thus do not allow precise ocular exposure to UVR without anesthesia. To overcome the adverse side effects of anesthesia and problems with available restraining devices, we built a rat restrainer that can immobilize unanesthetized rats at the ages of 6-18 weeks and allow accurate repeated *in vivo* exposures to optical radiation.

The restrainer is composed of a wooden base plate and three synthetic immobilization belts (Figure 5). The plate is attached with two bolts to a steel bar that is fixed to a tripod. The surface of the wooden base plate is smooth to prevent damage to the animal.

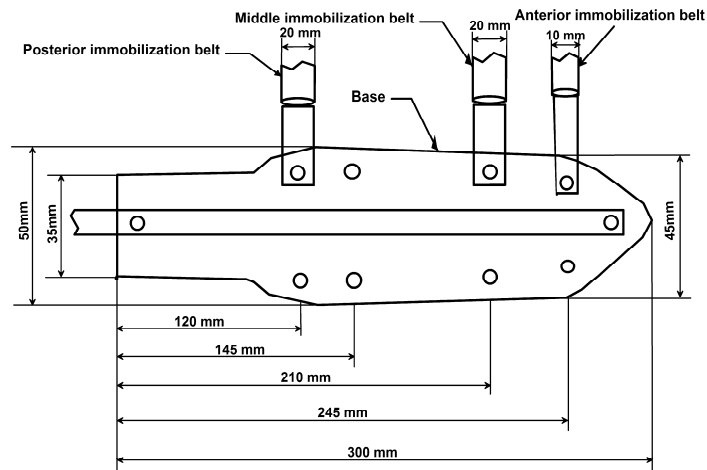


Figure 5. Schematic diagram of the rat restrainer.

Each immobilization belt consists of a fixed band and an opposing detachable band (Figure 6). The fixed band attaches at one end to the wooden base and distally ends in a metal loop. The opposing detachable band attaches with a metal clip to the wooden base plate. The distal end of the detachable band goes over the rat and slides through the metal loop at the distal end of the fixed band and is then attached to its origin with a Velcro fastener allowing for various rat sizes.

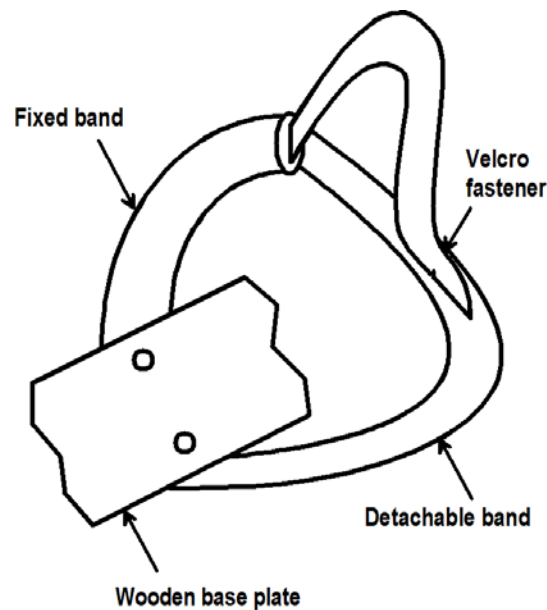


Figure 6. Schematic diagram of the immobilization belt.

While the rat is held with one hand, another hand fastens the belts over the animal's trunk. The anterior immobilization belt goes around the neck, the middle belt goes around the body behind the forelimbs, and the posterior belt goes around the body in front of the hind limbs (Figure 7). The head is further fixed with a leather collar over the maxilla and with two side strings pulling

backward, similar to horse reins, towards the attachment on the wooden base plate (Figure 8). The design allows one person to immobilize the rat without squeezing the animal's trunk.

Before exposure, the eyelids of the exposed eye are moved apart by paper strips attached to the eyelids with chewing gum at one end and a weight in the form of loaded paper clips at the other end of the strip (Figure 8).

This rat restrainer was used in all four studies.



Figure 7. Rat restrainer.



Figure 8. Maxilla collar.

3.3 UVR SOURCE

The same UVR source was used in all studies. UVR-B at 300 nm was generated with a high-pressure mercury arc lamp (model 6828; Oriel, Stratford, CT, USA). The emitted radiation was collimated, passed through a water filter, focused onto a double monochromator (model 77250, Oriel, USA) and projected as a narrow beam on the cornea of the exposed eye (Figure 9).

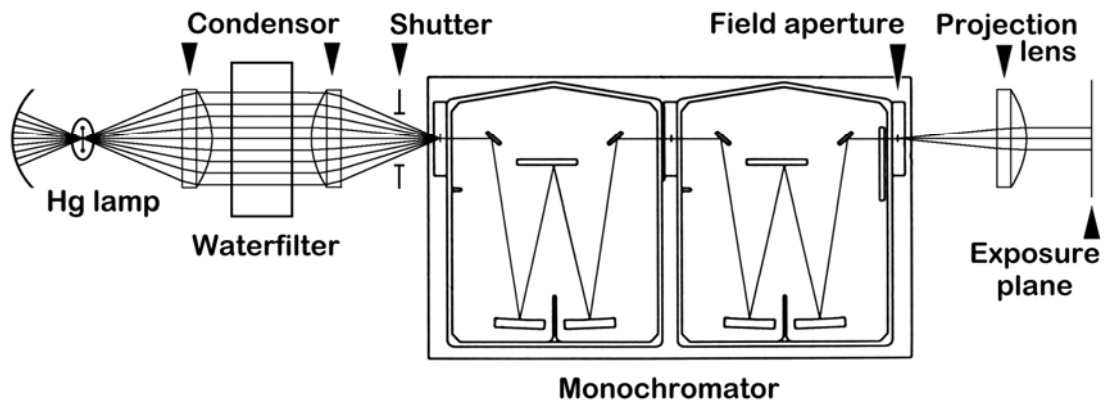


Figure 9. Schematic diagram of the UVR source.
(Reprinted with permission from Ralph Michael.
Development and Repair of Cataract Induced by Ultraviolet
Radiation. *Ophthalmic Research* 2000; February (suppl): 7.
Copyright by S. Karger, Basel).

The emerging radiation was recorded with a spectrometer (Ocean Optics PC 2000; Ocean Optics, Dunedin, Florida, USA) and had a spectrum centered at 300 nm with dual peaks at 297.5 nm and 302.6 nm with 10.2 nm full width at half maximum (Figure 10).

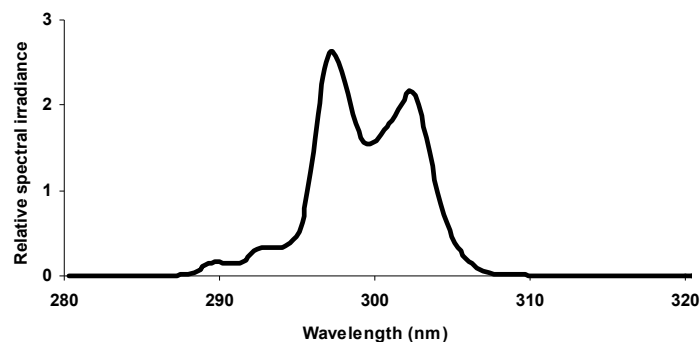


Figure 10. Spectral irradiance of the UVR source.

The intensity of UVR was measured with a thermopile (model 7101; Oriel, Stratford, CT, USA) calibrated to a US National Institute of Standards and Technology traceable source. The thermopile senses the temperature gradient produced by UVR-B absorption and converts the thermal energy of UVR-B to a voltage. Irradiance of UVR-B was controlled before and after each animal experimental exposure.

3.4 LENS DISSECTION

The enucleated eye was placed cornea down and posterior side up on a soft tissue. Under a dissecting microscope, the sclera was punched with a 27-gauge needle to make a hole. The sclera then was cut circumferentially just behind the limbus until a scleral flap could be lifted off. The lens was lifted using a blunt curved forceps and was then placed into balanced salt solution. The remnants of the ciliary body and vitreous body were then removed from the lens. The lens was never kept in balanced salt solution for longer than 10 minutes because this can cause lens opacification.

3.5 LIGHT DISSEMINATION METER

A light dissemination meter (LDM) was used to measure the degree of cataract and quantified as lens forward light scattering. The LDM instrument was built and developed by Söderberg (Söderberg et al., 1990). This instrument uses the principle of dark-field illumination (Figure 11).

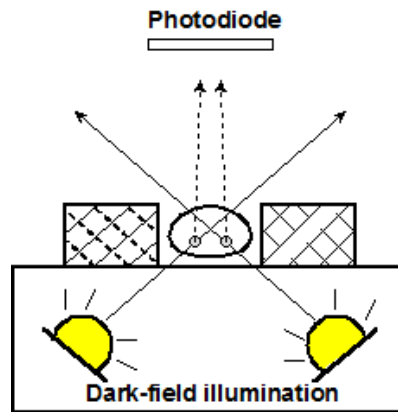


Figure 11. Principle of measurement of forward light scattering in the lens.

The illuminating light from a cold light source was directed toward the surface of the rat lens at 45° against the horizontal plane. At this angle, the light cannot enter the optics of the photometry unit if the lens is transparent. If the rat lens scatters light in the forward direction, a fraction of the scattered light is collected by the optics and projected onto a photodiode that produces a current proportional to the intensity of light incident on the surface of the photodiode. If the lens is totally opaque, the probing light is attenuated by absorption and back scattering.

The mean of three current readings for each lens was calibrated to the opacity standard, a commercially available lipid emulsion of diazepam (Stesolid Novum, Dumex-Alpha, Denmark). Light scattering was therefore expressed in equivalent diazepam concentration (EDC). EDC readings are not normally distributed (Söderberg et al., 1990). For application of parametric statistical methods normally distributed data is required. Therefore, the EDC readings were log transformed for normalization (tEDC) (Söderberg et al., 1990).

3.6 MACROPHOTOGRAPHY

Macrophotography was used to capture morphological changes in the lens after exposure to UVR-B. Macrophotography was used in studies II and III. Incident bright-field illumination against a white grid and dark-field illumination against a dark background were utilized (Figure 12).

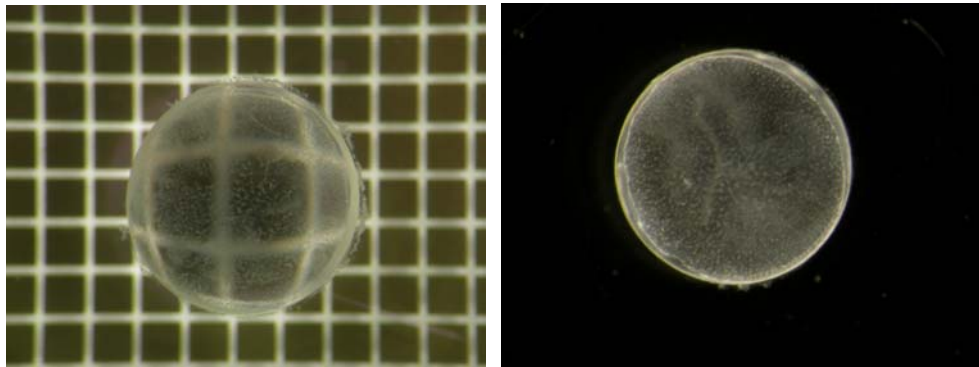


Figure 12. Macrophotographs of UVR exposed rat lenses in bright-field illumination against a white grid (left) and dark-field illumination against a dark background (right).

In bright-field illumination, the light originates from a paraxial cold light ring illuminating the lens from above. The light is incident through the crystalline lens to the white grid. Scattering is viewed as white spots against the dark surface lined by the white grid. In dark-field illumination, the light comes from beneath to the surface of the lens at an angle. Scattering is viewed as white spots in the lens against nothing. Local refractive index deviations are visible in bright-field illumination as local deviations of the white grid but not in dark-field illumination. The period size of the grid is 0.79 mm.

3.7 LIGHT AND TRANSMISSION ELECTRON MICROSCOPY

Light and transmission electron microscopy (TEM) were used in study II to investigate morphological changes accompanying apoptosis in the lens after exposure to UVR-B. Tissue preparation for TEM includes *fixation*, *dehydration* and *embedding in resin*.

Glutaraldehyde is the most commonly used primary fixative. It penetrates rapidly and stabilizes proteins by forming cross-links, but does not fix lipids. *Osmium tetroxide* is used as a secondary fixative, reacting with lipids and acting as a stain. Following each fixation step, excess fixative must be washed out of the tissue. Before the sample can be transferred to the resin, all the water must be removed from the sample. The dehydration step is performed using a graded ethanol series.

3.7.1 Protocol used for preparation for transmission electron microscopy

Lenses were fixated in Eppendorf tubes.

1. *Primary fixation*

Lenses were fixated in a 0.08 M cacodylate-buffered solution of 1.25% glutaraldehyde (G5882; Sigma-Aldrich, Sweden) and 1% paraformaldehyde (pH 7.3) for at least 7 days at 4°C. Notes: For primary fixation with aldehyde fixatives, the pieces were no larger than 3 mm³. If the lens pieces were larger, then smaller cubes 1.5 mm³ were cut before secondary fixation with osmium tetroxide. The fixative was at least 10 times greater in volume than the specimen.

2. *Washing.*

Lenses were washed in 0.1 M sodium cacodylate buffer for 2 hours or overnight at 4°C, pH 7.3. Notes: The specimen can be kept in the buffer for 3-5 days at 4°C.

3. *Lens dissection.*

Lenses were dissected into two similar halves with a sharp razor blade, and furthermore into smaller halves, to maximum 2 mm² and 3 mm as the longest dimension (six specimens per lens) (Figure 13).

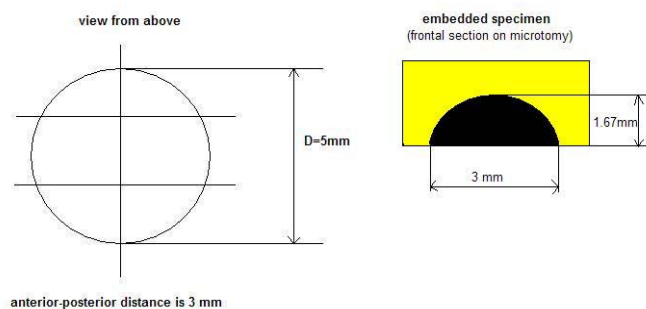


Figure 13. Lens dissection before secondary fixation with osmium tetroxide.

4. *Secondary fixation.*

Lenses were post-fixed in a 0.1 M cacodylate buffered solution of 1% osmium tetroxide (393517; Sigma-Aldrich, Sweden) supplemented with 1.5% potassium ferricyanide (393517; Sigma-Aldrich, Sweden) for 1 hour at 4°C.

Notes: Work was carried out in a vented hood. Double gloves were worn. The solution of osmium tetroxide had to be neutralized by double the volume of corn oil.

5. *Washing.*

Lenses were washed in 0.1 M sodium cacodylate buffer for 10 min twice at 4°C.

6. *Dehydration at 4°C.*

50% ethanol – overnight,

70% ethanol – 15 min,

90% ethanol – 15 min,

100% ethanol – 2x15 min.

7. *Embedding in epoxy resin.*

a) The epoxy resin was prepared by mixing the agar resin 100 (4.8 g), DDSA (dodecenyl succinic anhydride) (2.6 g), MNA (methyl nadic anhydride) (2.6 g) and BDMA (benzyl dimethylamine) (0.2 g).

b) The 50/50 propylene oxide/epoxy resin solution was prepared.

c) Ethanol from the lenses was removed and the propylene oxide (solvent) was added for 2x10 min.

d) Lens pieces were placed in 50/50 propylene oxide/epoxy resin for 3 hours.

e) Lens pieces were left in the epoxy resin overnight with the caps removed from the Eppendorf tubes at room temperature. This allowed any residual propylene oxide to evaporate.

f) Next day! Paper ID notes were placed at the bottom of embedding molds, in the non-sectioning end, with the pencil text upwards. The lens specimens were placed to the sectioning end. Epoxy resin was filled in the molds until a flat surface is achieved.

g) Epoxy resin in the embedding mold was polymerized at 60°C for 24 hours or up to three days. Double gloves were worn.

Semi-thin sections (500 nm thick) of the embedded lens tissue were stained with 1% toluidine blue for light microscopy. Ultrathin sections (80 nm thick) were obtained and mounted on parallel bar copper grids (200MP, Cat # G200P; Electron Microscopy Sciences). The sections were then double stained in 3.5% uranyl acetate for 20 minutes at room temperature, followed

by Reynold's lead citrate for 10 minutes at room temperature. The grids with sections were examined in a Tecnai G2 Bio Twin Spirit (FEI Company, USA) transmission electron microscope. The resolution of modern TEM has achieved 50 pm while light microscopy can resolve objects 0.2 μm apart.

3.8 QUANTITATIVE REVERSE TRANSCRIPTION POLYMERASE CHAIN REACTION (QRT-PCR)

qRT-PCR is a very sensitive method of modern molecular biology that allows the detection of very low amounts of RNA in a sample. qRT-PCR was used in the mRNA evolution study of p53, caspase3 and gadd45 α (paper IV).

RNA from each lens was isolated using a NucleoSpin RNA II kit (Macherey-Nagel GmbH & Co, Duren, Germany). Sufficient removal of DNA from the sample was checked by PCR under the following conditions (step 1: 95°C for 2 min; step 2 for 40 cycles: 95°C for 20 sec, 55°C for 20 sec, 72°C for 20 sec; step 3: 72°C for 7 min) using p53 DNA specific primers, forward 5'-ACCCTCTGACCTTTTCCCA-3' and reverse 5'-TGCTGGGATCTTAGGCACTC-3' (biomers.net GmbH, Ulm, Germany), and Taq DNA polymerase (dNTPack), according to the manufacturer's protocol. The expected PCR product was 243 base pairs. DNA-specific PCR products were visualized by agarose gel electrophoresis. If samples contained DNA, the RNA isolation protocol with the NucleoSpin RNA II kit was run again.

The RNA concentration and the ratio of sample absorbance at 260 nm (RNA) and 280 nm (protein) in the sample were measured using a NanoDrop ND-1000 spectrophotometer (NanoDrop Products, Wilmington, DE, USA). If the ratio of RNA to protein of an RNA sample absorbance was 2.0 or higher, the RNA sample was pure. If the ratio of RNA sample absorbance was lower than 2.0, the RNA purification step was performed again. A volume of RNA sample corresponding to 1 μg of total RNA was used to synthesize cDNA following the protocol (First Strand cDNA synthesis kit, Roche Diagnostics GmbH, Mannheim, Germany). In order to avoid degradation of cDNA, samples should be stored at -20°C for up to one year and at -70°C for longer periods.

The cDNA made from lens RNA was analyzed in triplicate by semi-quantitative real-time PCR on an iCycler MyiQ Single Color Real Time PCR detection system (Bio-Rad Laboratories, Hercules, CA, USA). Triplicates were loaded in 96-well plates (one plate for each target mRNA) with 1 µl of the cDNA sample, TaqMan Gene Expression Master Mix, TaqMan Gene Expression Assay for p53 (Rn00755717_m1), caspase 3 (Rn00563902_m1), gadd45α (Rn99999121_m1) or 18s (Hs99999901_s1), according to the manufacturer's instructions (TaqMan Gene Expression Assay Protocol, Applied Biosystems, Foster City, CA, USA). Primary fluorescence measurements were fitted with the MyiQ (Bio-Rad Laboratories, Hercules, CA, USA) algorithm and threshold fluorescence was standardized for each PCR plate by the algorithm. The number of cycles at threshold fluorescence was used as the measurement.

Measurements were quantified using the standard curve obtained by amplifying serially diluted samples of the cDNA of interest. First, a fraction of cDNA from three randomly chosen lenses was serially diluted. The serial dilutions were run together with the cDNA from samples. Second, a standard curve expressing the number of cycles at threshold, as a function of the relative concentration, was established for the serial dilutions in each plate. The PCR efficiency was estimated to an average of 90 %. Third, the number of cycles for each sample to reach the threshold was related to the standard curve to obtain the relative concentration of cDNA in the measured sample. Fourth, the expression level of the target genes TP53, CASP3 and GADD45α was determined by relating the relative concentration of the target cDNA to the internal control 18s cDNA. Finally, the fold-change in mRNA expression for the target gene in the lens after UVR exposure was calculated as the ratio between the expression level of the target gene in the exposed lens and the expression level of the target gene in the contralateral unexposed lens.

3.9 EXPERIMENTAL DESIGN (BY PAPERS)

- I. In the rat restrainer study, 83 6-week-old and three 18-week-old Sprague-Dawley female rats were included. Initially, each rat was conditioned to the rat restrainer for five days in accordance with the

following schedule: first two days – animals were placed in the rat restrainer for 5-15 min; days 3, 4 and 5 – animals were restrained for 5, 10 and 15 min, respectively. After restraining, animals were fed with apple to create a positive association with the procedure. Eighty 6-week-old rats were restrained and exposed to UVR-B for 15 min. Three 6-week-old rats and three 18-week-old rats were restrained and exposed to UVR-B for 15 min on 10 consecutive days. Signs of stress were recorded during behavioral work and exposure.

- II. In the study on the evolution of morphological changes in the lens after UVR-B exposure, eighty 6-week-old Sprague-Dawley female rats were randomly distributed into four latency groups with 20 animals in each, using a geometrical scale: 1, 7, 48 and 336 h. Before exposure, each animal was conditioned to the rat restrainer. One eye of each animal was exposed *in vivo* to UVR at 300 nm and the contralateral unexposed eye was kept as a control. In vitro macrophotography was taken for all lenses. The paired difference in lens forward light scattering between the exposed and unexposed lenses was measured with the light dissemination meter. Three exposed lenses and one unexposed lens from each time interval were studied with light and transmission electron microscopy.
- III. In the chronic exposure study, eighty 18-week-old Sprague-Dawley female rats were randomly distributed to four exposure period groups with 20 animals in each using a geometrical scale: 1, 3, 10 and 30 days of exposure to UVR-B. Each exposure period group was subdivided into five cumulated UVR dose subgroups with calculated exposure doses according to the $MTD_{2.3:16}$ concept (**Table 3**) (Dong et al., 2005).

Table 3. Daily doses with expected MTD_{2.3:16} 4.5 kJ/m².

Number of days exposed	Cumulative dose (kJ/m ²)				
	0.00	3.18	4.50	5.51	6.36
	Daily dose (kJ/m ²)				
1	0.00	3.18	4.50	5.51	6.36
3	0.00	1.06	1.50	1.84	2.12
10	0.00	0.32	0.45	0.55	0.64
30	0.00	0.11	0.15	0.18	0.21

All animals were conditioned to the rat restrainer before exposure. After daily exposures to UVR-B, the intensity of lens forward light scattering was measured three times for each lens. The MTD_{2.3:16} was estimated for the periods of exposure and plotted as a linear regression as a function of the length of the treatment period. Cataract morphology was documented with a microscope camera system.

- IV. In the study of the evolution of GADD45 α , TP53 and CASP3 gene expression in the lens after UVR-B exposure, forty 6-week-old Sprague-Dawley female rats were randomly distributed to four post-exposure groups with ten animals using a geometrical scale: 1, 5, 25 and 120 h. One eye of each anesthetized animal was exposed to UVR-B at 300 nm while the contralateral unexposed eye was used as a control. The expression level of the GADD45 α , TP53 and CASP3 genes in the rat lens after exposure to UVR-B was measured by qRT-PCR. 18s rRNA was used as the reference gene.

3.10 STATISTICAL PARAMETERS

Throughout the thesis, the significance levels and confidence coefficients were set to 0.05 and 0.95, respectively.

4 RESULTS AND DISCUSSION

4.1 PAPER I, RAT RESTRAINER STUDY

A new universal rat restrainer was developed (Galichanin et al., 2011). All rats were familiarized to the device with a tendency of young animals to accustom faster than older animals. Stress was recorded as any sign of urination, defecation, increased body movements and vocalization. Ten 6-week-old rats showed some signs of stress whereas 70 rats did not exhibit any signs of stress during single exposure to UVR-B. One 18-week-old rat revealed minor signs of stress initially, whereas two rats were well-conditioned to the procedure with repeated exposures to UVR-B. The group of 6-week-old rats adapted well to the 10 consecutive exposures.

Rats were restrained and exposed to UVR-B without the need for anesthetics. Animals successfully adapted to the restraining device. The learning of the experimental procedure could be due to non-associative learning, habituation, or associative learning, conditioning. Habituation refers to a reduction in responsiveness to a repeated stress stimulus. According to Thompson et al. (Thompson and Spencer, 1966) who formulated nine criteria of habituation, habituation occurs with repeated stimuli and is a reversible process. In the case of this study, repeated daily placement of the rat in the restrainer could possibly elicit habituation. It could also be that conditioning of the rat to the device was successful as the rat's response to the experimental procedure was reinforced with a subsequent apple reward. A more validated analysis of stress can be done by studying the decline of hypothalamic-pituitary-adrenal activation during repeated exposure to the same stressor.

The device is cheap to manufacture and easy to handle by one person. Rodent restraint with cage-type devices requires two people for handling (Lewis et al., 1989; Reich and Keller, 1988). In contrast to other devices such as cylinder (Pitts, 1976; Warden et al., 2000) and cable types (Rice and Ketterer, 1977) that permit head movement, our rat restrainer sufficiently immobilizes the animal and does not allow for head movements. The maxilla collar (Figure 8) resembles the function of horse reins by keeping the animal's head

steady in the straight position, thus allowing for precise ocular exposure to UVR-B and visible radiation. We previously learned in our laboratory that commercially available devices did not hold the animal's head steady.

Use of the newly developed device, with initial behavior adaption, allowed experimental exposure without anesthetics. Side effects in animals induced by anesthesia, such as acute transient lens opacities (Fraunfelder and Burns, 1970; Weinstock et al., 1958), respiratory and cardiovascular depression, polyuria and excessive defecation (Hsu et al., 1986; Wixson et al., 1987), have been reported. The combination of the anesthetic ketamine and the tranquilizer xylazine is a common combination used for narcosis in laboratory animals. Zhang et al. found that the combination of ketamine and xylazine causes transient cataract in rats that disappear within a few hours after the administration (Zhang et al., 2007). A previous study on acute reversible cataract concluded that the cause of this type of cataract is water evaporation from the corneal surface (Calderone et al., 1986). This phenomenon can disqualify measurements of the degree of cataract carried out several hours after the administration of anesthetics.

4.2 PAPER II, EVOLUTION STUDY OF APOPTOTIC MORPHOLOGICAL CHANGES IN THE LENS AFTER EXPOSURE TO UVR-B

The difference in forward light scattering between exposed and unexposed lenses increased towards an asymptote as a function of post-exposure time (Figure 14),

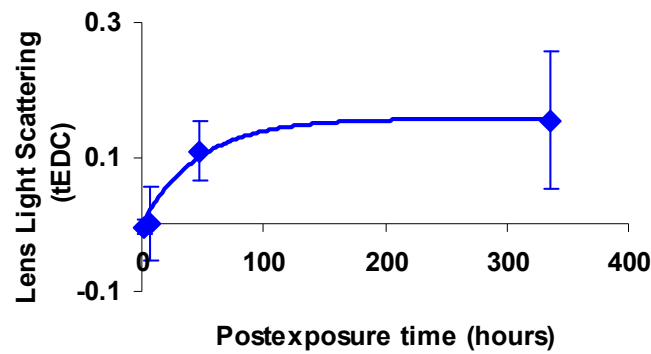


Figure 14. Mean paired differences in forward light scattering between exposed and unexposed lenses as a function of post-exposure time. Error bars are 95% confidence intervals for the mean. The line shows the best fit to an exponential regression model.

revealed by orthogonal t-tests between different post-exposure intervals. The increase in light scattering was best fit to a first order exponential regression model (Figure 14). The trend of an exponential increase in forward light scattering after exposure to 8 kJ/m^2 UVR-B in this study is similar to previous work by Söderberg (Söderberg, 1990) in which 30 kJ/m^2 was applied. Regardless of the method of immobilization, either using the rat restrainer in the current study or anesthesia in the earlier study, the exponential trend of light scattering development remained constant. However, the previous study documented a quicker onset of lens scattering than in the current study: an increase rate ($1/k$) of 0.05 h^{-1} (Söderberg, 1990) vs. an increase rate of 0.02 h^{-1} . In addition, the higher dose produced a higher maximum level of the difference in lens light scattering as 0.42 tEDC (Söderberg, 1990) in contrast to 0.16 tEDC in the current study. In conclusion, a higher UVR dose results in a higher level of lens opacification and a quicker early onset of light scattering in the lens.

Three animals belonging to the 336 hour group expressed a considerably larger difference in forward light scattering, between the exposed and unexposed lens, than all the other animals, $0.6\text{-}0.7 \text{ tEDC}$. In Figure 15, the differences between exposed and unexposed lens for animals belonging to the 336 hour group is presented.

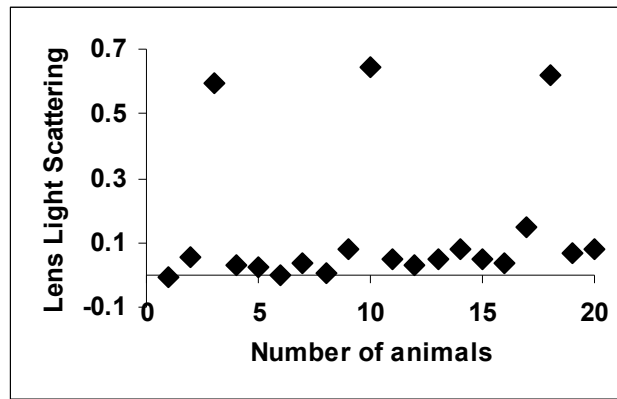


Figure 15. Plot of the difference in forward light scattering between exposed and contralateral unexposed lenses in the 336 h group of 20 rats.

The three rats with more expressed differences in light scattering exhibited severe cortical and nuclear cataract. Our group has previously reported cases of severe cataract after UVR-B exposure (Dong et al., 2003; Löfgren et al., 2003; Meyer et al., 2008; Meyer et al., 2005). It seems that variable sensitivity among animals, to develop cataract induced by UVR-B, could be due to differences in the capacity of the lens repair system. It was interesting that the three animals belonged to the 336 h group, leading to the hypothesis that there might be a critical time point between 48 h and 336 h for the lens repair system to restore UVR-B damage or to fail.

Acute reversible lens opacities induced by anesthetics (Calderone et al., 1986; Fraunfelder and Burns, 1970) could contribute to increased light scattering in the lens after UVR-B exposure (Zhang et al., 2007), but in the present study, we neglected transient cataract development by using the rat restrainer without anesthetics (Galichanin et al., 2011).

Light and transmission electron microscopy revealed that UVR damage in the lens begins in the lens epithelium, the first target for UVR photons, then spreads in an anterior-to-posterior direction along the length of the fiber cells and from superficial to deep lens fiber cells. The propagation of the osmotic disturbance between fiber cells in the lens cortex occurs via ion gap junctions (Kuszak et al., 1978). The lens epithelium exhibits apoptotic features after exposure to UVR-B and the lens cortex shows swollen and fused fiber cells with extracellular vacuoles. Extracellular vacuoles contain calcium, a major source of forward lens light scattering (Vrensen et al., 1995). The microscopic appearance of lens damage precedes the macroscopic appearance

of anterior subcapsular and cortical cataract. This is in accordance with an earlier study by Söderberg et al. (Söderberg, 1988) and observations of *in vitro* studies on cultured lenses (Li and Spector, 1996). Li et al. assayed apoptosis in the lens epithelium by TUNEL labeling and reported that apoptosis precedes the macroscopic appearance of anterior lenticular opacities (Li and Spector, 1996). Moreover, research in our group concluded that macroscopically visible flake-like lenticular opacities on the anterior surface of the lens are related to the distribution of apoptotic bodies in the lens epithelium (Michael et al., 2000).

The lens epithelium in the 336 h group recovered after UVR-B exposure. Lens epithelial cells in the central zone of the lens epithelium, which encompass 80 % of all lens epithelial cells, divide rarely because they are predominantly in the resting phase (G_0) in the cell cycle which can last for many years. However, the population of epithelial cells in the germinative zone divides and differentiates into fiber cells and also contributes to the population in the central zone. The induction of mitotic activity in epithelial cells in the germinative zone by UVR-B could explain the recovery of the lens epithelium observed 336 h after exposure.

4.3 PAPER III, CATARACT AFTER CHRONIC REPEATED EXPOSURES TO UVR-B

Current safety standards (ICNIRP et al., 2004) include experimental studies based on single UVR-B exposures with precise dosimetry (Pitts et al., 1977); (Söderberg, 1988); (Merriam et al., 2000), but scarce qualitative experimental studies are available on chronic repeated UVR-B exposures (Bachem, 1956; Jose and Pitts, 1985). Moreover, current guidelines consider that all damage in the lens is repaired within 24 hours. The aim of this study was to elucidate if subthreshold doses of UVR-B accumulate and cause cataract in the lens over a time period up to 30 days. This experimental design simulates the temporal pattern of natural daily solar UVR exposure in people's eyes.

Macroscopically, the lenses showed variable appearance of anterior subcapsular cataract depending on the exposure period group (Figure 16).

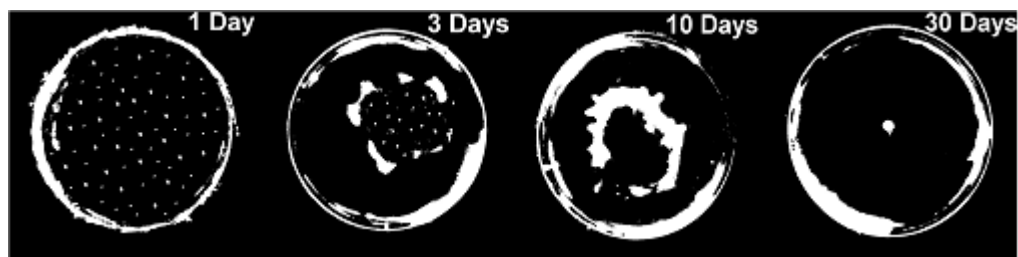


Figure 16. Appearance of cataracts (threshold images).

In the one day group, exposed lenses showed flake-like opacities all over the anterior surface of the lens. In the three days group, lens opacities were represented as an annulus with flake-like opacities. Flake-like opacities on the anterior surface of the lens could correspond to apoptotic changes occurring in the lens epithelium (Galichanin et al., 2010; Li and Spector, 1996; Michael et al., 2000). Lenses exposed for ten days showed an annulus on the anterior surface of the lens. Lenses exposed for 30 days exhibited anterior polar and equatorial cataracts. Annulus-like rough opacities and anterior polar cataracts could reflect the central migration of apical tips of damaged elongating fiber cells before they lose contact with the lens epithelium and form lens sutures (Bassnett and Beebe, 2004).

The paired difference in forward lens light scattering increased as a function of cumulated UVR-B dose in all exposure period groups. This finding is consistent with a continuous dose-response relationship for UVR-B induced cataract as was previously demonstrated for acute UVR induced cataract (Söderberg et al., 2003).

The $MTD_{2.3:16}$ for 1, 3, 10 and 30 days of repeated exposures were calculated to be 4.70, 4.74, 4.80 and 6.0 kJ/m^2 , respectively (Figure 17).

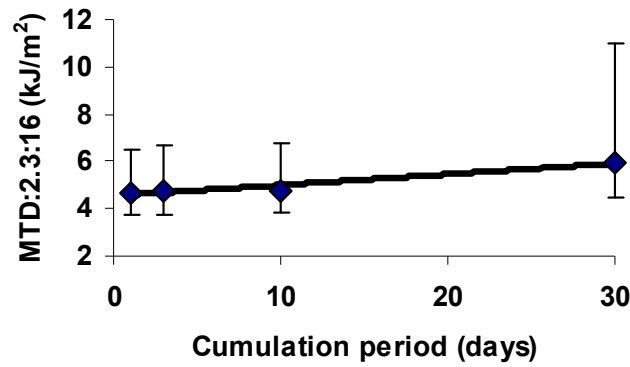


Figure 17. Lens threshold to UVR-B exposure expressed as increased MTD_{2.3:16} as a function of cumulative dose. Error bars are 95% confidence intervals for MTD_{2.3:16}. The line is the fit to the linear regression model.

The trend of MTD_{2.3:16} increases during daily exposures with increasing cumulation period (Figure 17), in other words decreasing daily UVR-B dose, implicates a repair mechanism in the lens. Such a repair will then reduce the damage in between each daily subthreshold exposure so that the cumulated damage is less than if the dose is delivered in one exposure. Therefore, lens damage after consecutive UVR-B exposures is defined by the repaired damage of antecedent exposure and the damage due to consecutive exposure (Dong et al., 2007). This should be considered for the understanding of damage in the lens from sunlight accumulated over a lifetime potentially manifesting as cataract at high age.

4.4 PAPER IV, EVOLUTION STUDY OF TP53, CASP3 AND GADD45A GENE EXPRESSION IN THE LENS AFTER *IN VIVO* EXPOSURE TO UVR-B

The study was designed to elucidate the kinetics of gene expression of the genomic damage sensor and repair gene (GADD45 α), a marker of early phase apoptosis (TP53) and late phase apoptosis (CASP3) in the lens after *in vivo* exposure to UVR-B.

GADD45 α was selected because it functions as a stress sensor (Liebermann and Hoffman, 2008) and nucleotide excision repair gene (Smith et al., 2000) for UVR. Caspase-3 is the main protease in the execution phase of apoptosis (Elmore, 2007). For this reason, caspase-3 was selected as a reliable marker

for apoptosis with a higher specificity than the TUNEL assay (Duan et al., 2003; Gown and Willingham, 2002; Walker and Quirke, 2001). The TUNEL assay recognizes DNA strand breaks in apoptotic cells. However, DNA strand breaks are not unique to apoptosis but also occur in necrosis and during the repair of DNA damage (Grasl-Kraupp et al., 1995). Additionally, we chose the TP53 gene because it is an initiator of apoptosis (Schuler and Green, 2001; Shen and White, 2001) and earlier investigations on UVR induced apoptosis in the lens concluded that apoptosis is p53-mediated (Ayala et al., 2007).

Orthogonal t-tests revealed a difference in the GADD45 α /18s ratios between 5 h and 24 h versus 1 h and 120 h (test statistic = 2.31, $t_{38, 0.975} = 2.02$) (Galichanin et al., 2012)(**Figure 18**). This transient increase between 5 h and 24 h after UVR-B exposure reflects the role of GADD45 α as a stress sensor and repair gene (Liebermann and Hoffman, 2008).

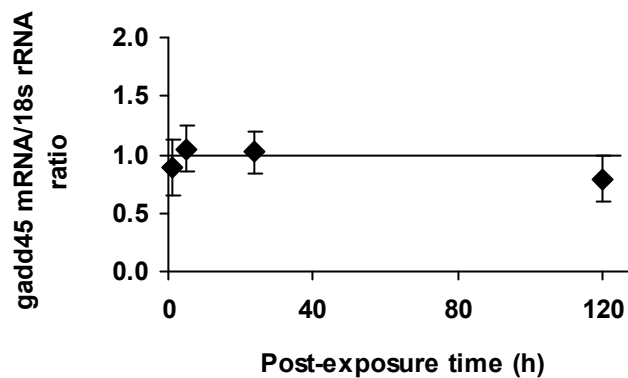


Figure 18. Evolution of GADD45 α mRNA expression in the crystalline lens after in vivo exposure to 8 kJ/m² UVR at 300 nm. Error bars are 95 % confidence intervals for mean ratio of gadd45 α mRNA/18s rRNA between exposed lens and contralateral unexposed lens.

An initial decrease in TP53 and CASP3 mRNA expression was seen in the lens after UVR-B, in accordance with another study that found a depression in mRNA synthesis after UVR exposure (Kantor and Hull, 1979). The time between UVR-B exposure and the onset of reactive mRNA transcription of the TP53 (24 h) and CASP3 (49 h) genes reflects the initial depression and recovery of mRNA synthesis (Figure 19).

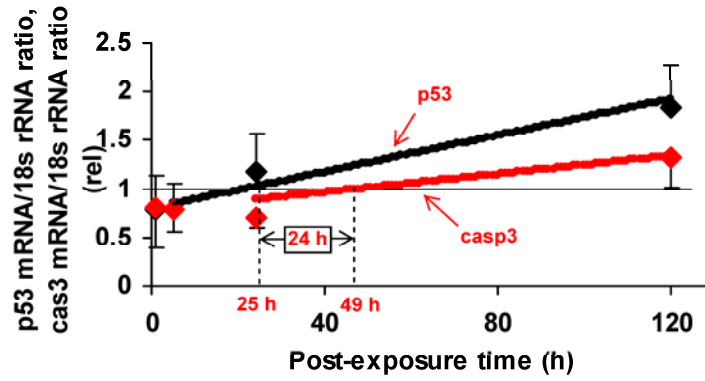


Figure 19. Time evolution of TP53 and CASP3 mRNA expression in the lens after *in vivo* exposure to 8 kJ/m² UVR at 300 nm. Error bars are 95% confidence intervals for the means. The black line at 1 rel. units shows no difference in the TP53/18s and CASP3/18s ratios between exposed and unexposed control lenses. The thick black and red lines show the best fit of TP53 and CASP3 mRNA expression to a straight line regression model, respectively.

Figure 19 shows that, after UVR-B exposure, the time gap between the recovery of TP53 transcription and recovery of CASP3 transcription in the lens is 24 h. This fits the general scheme of p53-dependent apoptosis where p53 is the initiator and caspase-3 is the executor of apoptotic events (Elmore, 2007). This finding, of a significant increase in p53 and caspase 3 mRNA expression at 120 h, is consistent with our group's previous study in which it was found that 7 days after UVR exposure p53 and caspase 3 mRNA are observed in the lens (Ayala et al., 2007).

Since the orthogonal t-tests indicated an increase in p53 and caspase-3 mRNA between exposed and unexposed contralateral lenses as a function of time after UVR-B exposure (Figure 19), the data were fitted to a straight line regression model with the estimated increase rate of mRNA synthesis for p53 and caspase-3 as 9.4×10^{-3} and 4.7×10^{-3} rel units/h, respectively (Figure 19). Here, the increased rate probably represents a true increase in transcription from the genome of the lens epithelial cells rather than transcription of amplified DNA as observed in cancer cells (Lockwood et al., 2008). A transcription of amplified DNA in cancer cells would implicate an exponential trend. Considering a true increase in transcription after UVR exposure, the increase rate probably reflects an increased integrated RNA polymerase activity.

5 CONCLUSIONS

- We developed a new universal rat restrainer that effectively immobilizes unanesthetized rats in the age range 6-18 weeks old. It allows daily well-controlled *in vivo* exposures of the eye to UVR and visible light.
- The higher the *in vivo* UVR dose, the quicker the development of lens opacification and the higher the degree of lens opacification. UVR-B exposure induces apoptosis in the lens epithelium, and the lens epithelium is the primary target of UVR exposure. Apoptotic events in the lens epithelium precede macroscopic cataractogenesis and occur within 48 hours after exposure to UVR-B. The lens epithelium repairs within 336 hours after exposure to 8 kJ/m² of UVR-B, whereas cortical fiber cells remain damaged.
- Subthreshold exposures of UVR-B accumulate in the rat lens and cause cataracts *in vivo*. MTD_{2,3,16} for 1, 3, 10 and 30 days of repeated exposures was estimated to be 4.70, 4.74, 4.80 and 6.00 kJ/m², respectively. Thus, the tolerance for daily subthreshold UVR-B exposures in 18-week-old Sprague-Dawley rats increases with the number of days of exposure.
- Double the threshold dose of UVR-B causes a transient upregulation in the stress sensor GADD45 α , a transient downregulation in TP53 and CASP3, followed by a constant upregulation of TP53 that precedes a constant upregulation of CASP3 in the rat lens *in vivo*.

6 REFERENCES

- Andley, U.P., Clark, B.A., 1989. Generation of Oxidants in the Near-UV Photooxidation of Human Lens α -Crystallin. *Investigative Ophthalmology and Visual Science* 30, 706-713.
- Andley, U.P., Walsh, A., Kochevar, I.E., Reddan, J.R., 1990. Effect of ultraviolet-B radiation on protein synthesis in cultured lens epithelial cells. *Current Eye Research* 9, 1099-1106.
- Ayala, M.N., 2005. Influence of exposure patterns and oxidation in UVR induced Cataract. Thesis. Karolinska Institutet, Stockholm.
- Ayala, M.N., Michael, R., Söderberg, P.G., 2000. Influence of exposure time for UV radiation-induced cataract. *Investigative Ophthalmology and Visual Science* 41, 3539-3543.
- Ayala, M.N., Strid, H., Jacobsson, U., Söderberg, P.G., 2007. p53 expression and apoptosis In The Lens After Ultraviolet Radiation Exposure. *Investigative Ophthalmology of visual science* 48, 4187-4191.
- Bachem, A., 1956. Ophthalmic ultraviolet action spectra. *American Journal of Ophthalmology* 41, 969-975.
- Bantsev, V., Youn, H.Y., 2006. Mitochondrial "movement" and lens optics following oxidative stress from. *Annals of the New York Academy of Sciences* 1091, 17-33.
- Bassnett, S., Beebe, D., 1992. Coincident loss of mitochondria and nuclei during lens fiber cell differentiation. *Developmental Dynamics* 194, 85-93.
- Bassnett, S., Beebe, D., 2004. Lens fiber differentiation, in: Lovicu, F.J., Robinson, M.L. (Eds.), *Development of the ocular lens*. Cambridge University Press, pp. 214-245.
- Boettner, E.A., Wolter, J.R., 1962. Transmission of ocular media. *Investigative Ophthalmology and Visual Science* 1, 776-783.
- Boyle, D.L., Carman, P., Takemoto, L., 2002. Translocation of macromolecules into whole rat lenses in culture. *Mol Vis* 8, 226-234.
- Brian, G., Taylor, H.R., 2001. Cataract blindness: challenge for the 21 st century. *Bulletin of the World Health Organization* 79, 249-256.
- Calderone, L., Grimes, P., Shalev, M., 1986. Acute reversible cataract induced by xylazine and by ketamine-xylazine anesthesia in rats and mice. *Experimental Eye Research* 42, 331-337.
- Caul, W.F., Buchanan, D.C., 1971. A restrainer for rat immobilization. *Physiology and Behavior* 7, 919-920.
- CIE, 1999. Standardization of the terms UV-A1, UV-A2, and UV-B. CIE collection of Photobiology and Photochemistry 134/1.
- Clarke, P.G., Clarke, S., 1996. Nineteenth century research on naturally occurring cell death and related phenomena. [Review] [143 refs]. *Anatomy and Embryology* 193, 81-99.
- Congdon, N.G., 2001. Prevention strategies for age related cataract: present limitations and future possibilities. *British Journal of Ophthalmology* 85, 516-520.
- Coroneo, M.T., Muller-Stolzenburg, N.W., Ho, A., 1991. Peripheral light focusing by the anterior eye and the ophthalmohelioses. *Ophthalmic Surgery* 22, 705-711.
- Coutts, A.S., Adams, C.J., La Thangue, N.B., 2009. p53 ubiquitination by Mdm2: a never ending tail? *DNA Repair (Amst)* 8, 483-490.
- Cruikshanks, K.J., Klein, B.E., Klein, R., 1992. Ultraviolet light exposure and lens opacities: the Beaver Dam Eye Study. *American Journal of Public Health* 82, 1658-1662.

- D' Alleinne, C.P., Mann, D.D., 1982. Evaluation of ketamine/xylazine anesthesia in the guinea pig: toxicological parameters. *Veterinary and Human Toxicology* 24, 410-412.
- Danysh, B.P., Duncan, M.K., 2009. The lens capsule. *Exp Eye Res* 88, 151-164.
- Dillon, J., Zheng, L., Merriam, J.C., Gaillard, E.R., 1999. The optical properties of the anterior segment of the eye: implications for cortical cataract. *Experimental Eye Research* 68, 785-795.
- Dong, X., 2005. Safety limit estimation for cataract induced by ultraviolet radiation. Thesis. Karolinska Institutet, Stockholm.
- Dong, X., Ayala, M., Löfgren, S., Söderberg, P.G., 2003. Ultraviolet radiation-induced cataract: age and maximum acceptable dose. *Investigative Ophthalmology and Visual Science* 44, 1150-1154.
- Dong, X., Löfgren, S., Ayala, M., Söderberg, P.G., 2005. Maximum tolerable dose for avoidance of cataract induced by ultraviolet radiation-B for 18 to 60 weeks old rats. *Experimental Eye Research* 80, 561-566.
- Dong, X., Löfgren, S., Marcelo, A., Söderberg, P.G., 2007. Maximum tolerable dose for avoidance of cataract after repeated exposure to ultraviolet radiation in rats. *Experimental Eye Research* 84, 200-208.
- Duan, W.R., Garner, D.S., Williams, S.D., Funckes-Shippy, C.L., Spath, I.S., Blomme, E.A., 2003. Comparison of immunohistochemistry for activated caspase-3 and cleaved cytokeratin 18 with the TUNEL method for quantification of apoptosis in histological sections of PC-3 subcutaneous xenografts. *J Pathol* 199, 221-228.
- Elmore, S., 2007. Apoptosis: a review of programmed cell death. *Toxicologic Pathology* 35.
- Fraunfelder, F.T., Burns, R.P., 1962. Production of unilateral reversible cataracts in the hamster. *Proceedings of the Society for Experimental Biology and Medicine* 110, 72-74.
- Fraunfelder, F.T., Burns, R.P., 1970. Acute reversible lens opacity: caused by drugs, cold, anoxia, asphyxia, stress, death and dehydration. *Experimental Eye Research* 10, 19-30.
- Galichanin, K., Löfgren, S., Bergmanson, J., Söderberg, P., 2010. Evolution of damage in the lens after in vivo close to threshold exposure to UV-B radiation: cytomorphological study of apoptosis. *Exp Eye Res* 91, 369-377.
- Galichanin, K., Svedlund, J., Söderberg, P., 2012. Kinetics of GADD45alpha, TP53 and CASP3 gene expression in the rat lens in vivo in response to exposure to double threshold dose of UV-B radiation. *Exp Eye Res* 97, 19-23.
- Galichanin, K., Wang, J., Löfgren, S., Söderberg, P., 2011. A new universal rat restrainer for ophthalmic research. *Acta Ophthalmol* 89, e67-71.
- Gorgels, T.G., van Norren, D., 1992. Spectral transmittance of the rat lens. *Vision Research* 32, 1509-1512.
- Gown, A.M., Willingham, M.C., 2002. Improved detection of apoptotic cells in archival paraffin sections: immunohistochemistry using antibodies to cleaved caspase 3. *J Histochem Cytochem* 50, 449-454.
- Grasl-Kraupp, B., Ruttkay-Nedecky, B., Koudelka, H., Bukowska, K., Bursch, W., Schulte-Hermann, R., 1995. In situ detection of fragmented DNA (TUNEL assay) fails to discriminate among apoptosis, necrosis, and autolytic cell death: a cautionary note. *Hepatology* 21, 1465-1468.
- Gray, D.F., 2008. The black body and its radiation, The observation and analysis of stellar photospheres, Third ed. Cambridge University Press, New York, pp. 118-125.
- Harding, C.V., Reddan, J.R., Unakar, N.J., Bagchi, M., 1971. The control of cell division in the ocular lens. *Int Rev Cytol* 31, 215-300.
- Hightower, K., Duncan, G., Dawson, A., Wormstone, I., Reddan, J., Dziedzic, D., 1999. Ultraviolet irradiation (UVB) interrupts calcium cell signaling in lens epithelial cells. *Photochemistry and Photobiology* 69, 595-598.

- Hightower, K., McCready, J., 1992. Mechanisms involved in cataract development following near-ultraviolet radiation of cultured lenses. *Current Eye Research* 11, 679-689.
- Hightower, K.R., 1995a. A review of the evidence that ultraviolet irradiation is a risk factor in cataractogenesis. [Review]. *Documenta Ophthalmologica* 3-4, 205-220.
- Hightower, K.R., 1995b. The role of the lens epithelium in development of UV cataract. [Review]. *Current Eye Research* 14, 71-78.
- Hightower, K.R., Reddan, J.R., McCready, J.P., Dziedzic, D.C., 1994. Lens epithelium: a primary target of UVB irradiation. *Experimental Eye Research* 59, 557-564.
- Hsu, W.H., Bellin, S.I., Dellmann, H.D., Hanson, C.E., 1986. Xylazine-ketamine-induced anesthesia in rats and its antagonism by yohimbine. *Journal of the American Veterinary Medical Association* 189, 1040-1043.
- Höglund, J., 1999. *Diplostomum spathaceum* larvae (Diplostomosis) (Digenea) in fish = Larves de *Diplostomum spathaceum* (Diplostomose) chez le poisson. Fiches d'identification des maladies et parasites des poissons, crustacés et mollusques = ICES Identification Leaflets for diseases and parasites of fish and shellfish. International Council for the Exploration of the Sea, 4 pp.
- ICNIRP, Sliney, D.H., Cesarini, J.P., De Gruijl, F.R., Diffey, B., Hietanen, M., Mainster, M., Okuno, T., Söderberg, P.G., Stuck, B., 2004. Guidelines on limits of exposure to ultraviolet radiation of wavelengths between 180 nm and 400 nm (incoherent optical radiation). *Health Physics* 87, 171-186.
- Jose, J.G., Pitts, D.G., 1985. Wavelength dependency of cataracts in albino mice following chronic exposure. *Experimental Eye Research* 41, 545-563.
- Kakar, M.K., Mody, V.C., Löfgren, S., Ayala, M., Söderberg, P.G., 2003. Estimation of a Safety Limit for Ultraviolet Radiation-B (UVR-B) Induced Cataract in an in vivo Pigmented Rat Model. *ARVO abstract* 44, 296-.
- Kamaev, P., Friedman, M.D., Sherr, E., Muller, D., Photochemical kinetics of corneal cross-linking with riboflavin. *Invest Ophthalmol Vis Sci* 53, 2360-2367.
- Kantor, G.J., Hull, D.R., 1979. An effect of ultraviolet light on RNA and protein synthesis in nondividing human diploid fibroblasts. *Biophys J* 27, 359-370.
- Kerr, J.F., Wyllie, A.H., Currie, A.R., 1972. Apoptosis: a basic biological phenomenon with wide-ranging implications in tissue kinetics. *British Journal of Cancer* 26, 239-257.
- Kleiman, N.J., Wang, R., Spector, A., 1990. Ultraviolet light induced DNA damage and repair in bovine lens epithelial cells. *Curr. Eye Res* 9, 1185-1193.
- Kufoy, E.A., Pakalnis, V.A., Parks, C.D., Wells, A., Yang, C.H., Fox, A., 1989. Keratoconjunctivitis sicca with associated secondary uveitis elicited in rats after systemic xylazine/ketamine anesthesia. *Experimental Eye Research* 49, 861-871.
- Kurosaka, K., Takahashi, M., Watanabe, N., Kobayashi, Y., 2003. Silent cleanup of very early apoptotic cells by macrophages. *J Immunol* 171, 4672-4679.
- Kuszak, J., Alcala, J., Maisel, H., 1980. The surface morphology of embryonic and adult chick lens-fiber cells. *Am J Anat* 159, 395-410.
- Kuszak, J., Costello, M., 2004. The structure of the vertebrate lens, in: Lovicu, F., Robinson, M. (Eds.), *Development of the ocular lens*. Cambridge University Press, Cambridge, pp. 71-118.
- Kuszak, J., Maisel, H., Harding, C.V., 1978. Gap junctions of chick lens fiber cells. *Exp Eye Res* 27, 495-498.
- Kuwabara, T., 1975. The maturation of the lens cell: a morphologic study. *Exp Eye Res* 20, 427-443.

- Levine, A.J., 1997. p53, the cellular gatekeeper for growth and division. *Cell* 88, 323-331.
- Lewis, A., Long, A., Griffiths, R., 1989. New versatile Restraining device for use with rats in pharmacokinetic or pharmacological studies involving chronically implanted cannulae or electrodes. *J. Pharmacol. Meth.* 22, 59-63.
- Li, W.C., Kuszak, J.R., Dunn, K., Wang, R.R., Ma, W., Wang, G.M., Spector, A., Leib, M., Cotiar, A.M., 1995. Lens epithelial cell apoptosis appears to be a common cellular basis for non-congenital cataract development in humans and animals. *Journal of Cell Biology* 130, 169-181.
- Li, W.C., Spector, A., 1996. Lens epithelial cell apoptosis is an early event in the development of UVB-induced cataract. *Free Radical Biology and Medicine* 20, 301-311.
- Liebermann, D.A., Hoffman, B., 2008. Gadd45 in stress signaling. *J Mol Signal* 3, 15.
- Lockwood, W.W., Chari, R., Coe, B.P., Girard, L., Macaulay, C., Lam, S., Gazdar, A.F., Minna, J.D., Lam, W.L., 2008. DNA amplification is a ubiquitous mechanism of oncogene activation in lung and other cancers. *Oncogene* 27, 4615-4624.
- Lovicu, F.J., McAvoy, J.W., 2005. Growth factor regulation of lens development. *Dev Biol* 280, 1-14.
- Löfgren, S., Michael, R., Söderberg, P.G., 2003. Impact of age and sex in ultraviolet radiation cataract in the rat. *Investigative Ophthalmology and Visual Science* 44, 1629-1633.
- Löfgren, S., Michael, R., Söderberg, P.G., 2012. Impact of iris pigment and pupil size in ultraviolet radiation cataract in rat. *Acta Ophthalmol* 90, 44-48.
- Madronich, S., McKenzie, R.L., Bjorn, L.O., Caldwell, M.M., 1998. Changes in biologically active ultraviolet radiation reaching the Earth's surface. *J Photochem Photobiol B* 46, 5-19.
- Marchenko, N.D., Wolff, S., Erster, S., Becker, K., Moll, U.M., 2007. Monoubiquitylation promotes mitochondrial p53 translocation. *EMBO J* 26, 923-934.
- Marietta, M.P., White, P.F., Pudwill, C.R., Way, W.L., Trevor, A.J., 1976. Biodisposition of ketamine in the rat: self-induction of metabolism. *Journal of Pharmacology and Experimental Therapeutics* 196, 536-544.
- McCarty, C.A., Taylor, H.R., 2002. A review of the epidemiologic evidence linking ultraviolet radiation and cataracts. *Dev Ophthalmol* 35, 21-31.
- Mecherikunnel, A.T., Gatlin, J.A., Richmond, J.C., 1983. Data on total and spectral solar irradiance. *Appl Opt* 22, 1354.
- Merriam, J., Löfgren, S., Michael, R., Söderberg, P.G., Dillon, J., Zheng, L., Ayala, M., 2000. An action spectrum for UV-B radiation in the rat lens. *Investigative Ophthalmology and Visual Science* 41, 2642-2647.
- Meyer, L., Dong, X., Wegener, A., Söderberg, P.G., 2008. Dose dependent cataractogenesis and Maximum Tolerable Dose (MTD 2.3:16) for UVR - B induced cataract in C57BL/6J mice. *Experimental Eye Research* 86, 282-289.
- Meyer, L.M., Söderberg, P., Dong, X., Wegener, A., 2005. UVR-B induced cataract development in C57 mice. *Experimental Eye Research* 81, 389-394.
- Michael, R., Söderberg, P., Chen, E., 1998a. Dose response function for forward light scattering after in vivo exposure to ultraviolet radiation. *Graefes Archive for Clinical and Experimental Ophthalmology* 236, 625-629.
- Michael, R., van Marle, J., Vrensen, G.F., van den Berg, T.J., 2003. Changes in the refractive index of lens fibre membranes during maturation--impact on lens transparency. *Exp Eye Res* 77, 93-99.
- Michael, R., Vrensen, G., van Marle, J., Gan, L., Söderberg, P.G., 1998b. Apoptosis in the rat lens after in vivo threshold dose ultraviolet

- irradiation. *Investigative Ophthalmology and Visual Science* 13, 2681-2687.
- Michael, R., Vrensen, G.F.J.M., Marle, J.V., Löfgren, S., Söderberg, P.G., 2000. Repair in the rat lens after threshold ultraviolet radiation injury. *Investigative Ophthalmology and Visual Science* 41, 204-212.
- Mir, S., Wheatley, H.M., Hussels, I.E., Whittum-Hudson, J.A., Traboulsi, E.I., 1998. A comparative histologic study of the fibrillin microfibrillar system in the lens capsule of normal subjects and subjects with Marfan syndrome. *Invest Ophthalmol Vis Sci* 39, 84-93.
- Mody, V.C., 2008. Ultraviolet Radiation Cataract. Development and ascorbate supplementation. Thesis. Karolinska University Press, Stockholm.
- Mody, V.C., Jr., Kakar, M., Söderberg, P.G., Löfgren, S., 2012. High lenticular tolerance to ultraviolet radiation-B by pigmented guinea-pig; application of a safety limit strategy for UVR-induced cataract. *Acta Ophthalmol* 90, 226-230.
- Pitts, D., Cameron, L.L., Jose, J.G., 1986. Optical radiation and cataracts, Optical radiation and visual health. CRC Press, Boca Raton, Florida, pp. 5-41.
- Pitts, D.G., 1990. Sunlight as an Ultraviolet Source. *Optometry and Vision Science* 67, 401-406.
- Pitts, D.G., Cullen, A.P., Hacker, P.D., 1977. Ocular effects of ultraviolet radiation from 295 to 365 nm. *Investigative Ophthalmology and Visual Science* 16, 932-939.
- Pitts, W.G., 1976. Rodent restrainer for biomicroscopy. *American Journal of Optometry and Physiological Optics* 53, 154-155.
- Rafferty, N.S., Rafferty, K.A., Jr., 1981. Cell population kinetics of the mouse lens epithelium. *J Cell Physiol* 107, 309-315.
- Reich, D.J., Keller, S.E., 1988. An improvement on the Bollman method of restraining and collecting thoracic duct lymph from the rat. *J. Immunol. Meth.* 110, 179-181.
- Rice, D.P., Ketterer, D.J., 1977. Restrainer and cell for dermal dosing of small laboratory animals. *Laboratory Animal Science* 27, 72-75.
- Riley, T., Sontag, E., Chen, P., Levine, A., 2008. Transcriptional control of human p53-regulated genes. *Nat Rev Mol Cell Biol* 9, 402-412.
- Sasaki, H., Kawakami, Y., Ono, M., Jonasson, F., Shui, Y.B., Cheng, H.M., Robman, L., McCarty, C., Chew, S.J., Sasaki, K., 2003. Localization of cortical cataract in subjects of diverse races and latitude. *Invest Ophthalmol Vis Sci* 44, 4210-4214.
- Schuler, M., Green, D.R., 2001. Mechanisms of p53-dependent apoptosis. *Biochemical Society Transactions* 29, 684-688.
- Shen, S.C., Yang, C.H., Lin, H.C., Chen, S.N., 2007. Aggressive small choroidal melanoma presenting as a dense cataract. *J Cataract Refract Surg* 33, 336-338.
- Shen, Y., White, E., 2001. p53-dependent apoptosis pathways. *Advances in Cancer Research* 82, 55-84.
- Shestopalov, V.I., Bassnett, S., 1999. Exogenous gene expression and protein targeting in lens fiber cells. *Invest Ophthalmol Vis Sci* 40, 1435-1443.
- Shestopalov, V.I., Bassnett, S., 2000. Expression of autofluorescent proteins reveals a novel protein permeable pathway between cells in the lens core. *Journal of Cell Science* 113, 1913-1921.
- Sliney, D.H., 1986. Physical factors in cataractogenesis: Ambient ultraviolet radiation and temperature. *Investigative Ophthalmology and Visual Science* 27, 781-790.
- Smith, M.L., Ford, J.M., Hollander, M.C., Bortnick, R.A., Amundson, S.A., Seo, Y.R., Deng, C.X., Hanawalt, P.C., Fornace, A.J., Jr., 2000. p53-mediated DNA repair responses to UV radiation: studies of mouse cells lacking p53, p21, and/or gadd45 genes. *Mol Cell Biol* 20, 3705-3714.
- Solomon, J.D., Shields, C.L., Shields, J.A., Eagle, R.C., Jr., 2011. Posterior capsule opacity as initial manifestation of metastatic cutaneous melanoma. *Graefes Arch Clin Exp Ophthalmol* 249, 127-131.

- Soussi, T., Beroud, C., 2001. Assessing TP53 status in human tumours to evaluate clinical outcome. *Nat Rev Cancer* 1, 233-240.
- Streeten, B.W., 1977. The zonular insertion: a scanning electron microscopic study. *Invest Ophthalmol Vis Sci* 16, 364-375.
- Söderberg, P.G., 1988. Acute cataract in the rat after exposure to radiation in the 300 nm wavelength region. A study of the macro-, micro- and ultrastructure. *Acta Ophthalmol. (Copenh.)* 66, 141-152.
- Söderberg, P.G., 1990. Development of light dissemination in the rat lens after exposure to radiation in the 300 nm wavelength region. *Ophthalmic Research* 22, 271-279.
- Söderberg, P.G., Chen, E., Lindström, B., 1990. An objective and rapid method for the determination of light dissemination in the lens. *Acta Ophthalmol. (Copenh.)* 68, 44-52.
- Söderberg, P.G., Löfgren, S., Ayala, M., Dong, X., Kakar, M., Mody, V., 2002. Toxicity of ultraviolet radiation exposure to the lens expressed by maximum tolerable dose (MTD). *Developments in Ophthalmology* 35, 70-75.
- Söderberg, P.G., Michael, R., Merriam, J.C., 2003. Maximum acceptable dose of ultraviolet radiation: a safety limit for cataract. *Acta Ophthalmologica Scandinavica* 81, 165-169.
- Söderberg, P.G., Philipson, B.T., Lindström, B., 1986. Unscheduled DNA synthesis in lens epithelium after in vivo exposure to UV radiation in the 300 nm wavelength region. *Acta Ophthalmol. (Copenh.)* 64, 162-168.
- Taylor, H.R., West, S.K., Rosenthal, F.S., Munoz, B., Newland, H.S., Abbey, H., Emmett, E.A., 1988. Effect of ultraviolet radiation on cataract formation. *New England Journal of Medicine* 319, 1429-1433.
- Thompson, R.F., Spencer, W.A., 1966. Habituation: a model phenomenon for the study of neuronal substrates of behavior. *Psychol Rev* 73, 16-43.
- Thylefors, B., 2001. Eye and vision research for the prevention of blindness - A global perspective. Special recognition award, ARVO 2001.
- Walker, J.A., Quirke, P., 2001. Viewing apoptosis through a 'TUNEL'. *J Pathol* 195, 275-276.
- Wang, J., Löfgren, S., Dong, X., Galichanin, K., Söderberg, P.G., 2010. Evolution of light scattering and redox balance in the rat lens after in vivo exposure to close-to-threshold dose ultraviolet radiation. *Acta Ophthalmol* 88, 779-785.
- Warden, S.J., Bennell, K.L., McMeeken, J.M., Wark, J.D., 2000. A technique for restraining rodents during hindlimb interventions. *Contemp Top Lab Anim Sci.* 39, 24-27.
- Weinstock, M., Stewart, H.C., Butterworth, K.R., 1958. Lenticular effect in mice of some morphine-like drugs. *Nature* 182, 1519-1520.
- Verdebout, J., 2010. Estimating natural UV personal exposure with radiative transfer calculations. *Radiat Prot Dosimetry* 141, 275-282.
- West, S.K., Longstreth, J.D., Munoz, B.E., Pitcher, H.M., Duncan, D.D., 2005. Model of risk of cortical cataract in the US population with exposure to increased ultraviolet radiation due to stratospheric ozone depletion. *Am J Epidemiol* 162, 1080-1088.
- West, S.K., Valmadrid, C.T., 1995. Epidemiology of risk factors for age-related cataract. *Survey of Ophthalmology* 39, 323-334.
- Wixson, S.K., White, W.J., Hughes, H.C., Jr., Lang, C.M., Marshall, W.K., 1987. The effects of Pentobarbital, Fentanyl-Droperidol, Ketamine-Xylazine and Ketamine-Diazepam on Arterial Blood pH, Blood Gases, Mean Arterial Blood Pressure and Heart Rate in Adult Male Rats. *Laboratory Animal Science* 37, 736-742.
- Vrensen, G.F.J.M., Sanderson, J., Willekens, B., Duncan, G., 1995. Calcium localization and ultrastructure of clear and pCMPS-treated rat lenses. *Investigative Ophthalmology and Visual Science* 36, 2287-2295.
- Zhang, F., Löfgren, S., Söderberg, P.G., 2007. Interaction of anesthetic drugs and UVR-B irradiation in the anterior segment of the rat eye. *Acta Ophthalmologica Scandinavica* 85, 745-752.

- Zhuang, S.M., Shvarts, A., van Ormondt, H., Jochemsen, A.G., van der Eb, A.J., Noteborn, M.H., 1995. Apoptin, a protein derived from chicken anemia virus, induces p53-independent apoptosis in human osteosarcoma cells. *Cancer Res* 55, 486-489.
- Zigman, S., 1985. Photobiology of the lens, In: *The ocular lens. Structure, function and pathology*. Marcel Dekker, New York, pp. 301-347.
- Zigman, S., Griess, G., Yulo, T., Schultz, J., 1973. Ocular protein alterations by near UV light. *Experimental Eye Research* 15, 255-264.